

# OERA Research on Tidal Marine Energy

## Sensor Testing Research for Environmental Effects Monitoring (STREEM)

### FINAL PROJECT REPORT

#### Project Leads:

Acadia University - Dr Brian Sanderson & Dr Anna Redden

#### Collaborators:

Luna Ocean & Sustainable Marine Energy

Project Number: 300-216

Project Commenced: 1 October 2018

Project Final Report Submitted: 30 June 2019

### ACER Technical Report No. 127

#### Citation:

Sanderson, BG, MJ Adams and AM Redden. 2019. Sensor Testing Research for Environmental Effects Monitoring (STREEM). Final Report to the Offshore Energy Research Association of Nova Scotia. Acadia Centre for Estuarine Research, Technical Report No. 127, 68 pp. Acadia University, Wolfville, NS, Canada.



# Sensor Testing Research for Environmental Effects Monitoring (STREEM)

Brian G. Sanderson, Mike J. Adams and Anna M. Redden  
Acadia Centre for Estuarine Research  
Acadia University

ACER Technical Report #127

June 30, 2019

## Contents

<b>1</b>	<b>Executive Summary</b>	<b>3</b>
<b>2</b>	<b>Introduction</b>	<b>5</b>
<b>3</b>	<b>Target detection by imaging sonar and camera</b>	<b>7</b>
3.1	Boat mounted imaging sonar and target-drifter . . . . .	7
3.1.1	13 October 2018 . . . . .	8
3.1.2	19 October 2018 . . . . .	12
3.2	Imaging sonars and optical cameras mounted to PLAT-I . . . . .	18
3.2.1	Target tracking on 23 October 2018 . . . . .	21
3.2.2	Sonar/camera fish detection at PLAT-I . . . . .	29
3.2.3	Target tracking across the central hull, 24 October 2018 . . . . .	31
3.2.4	Rotating the Gemini 720is, 24 October 2018 . . . . .	31
3.2.5	A configuration for effective monitoring of fish-turbine interaction . . . . .	33
<b>4</b>	<b>Interactions of active and passive acoustic devices</b>	<b>36</b>
4.1	Drifting hydrophone array with sonar (on/off): interference . . . . .	36
4.1.1	Comparison with hydrophones on the OpenHydro platform . . . . .	40
4.1.2	Vemco tag: 180 kHz PPM signal . . . . .	41
4.1.3	Vemco tag: 170 kHz HR signal . . . . .	41
4.1.4	Detection of a Transmitting Vemco Tag by Gemini 720is . . . . .	42
4.1.5	Performance of a Vemco HR2 Receiver with an operating Gemini 720is . . . . .	43
4.2	Vessel-mounted hydrophone(s) . . . . .	45
4.2.1	Performance of Vemco HR2 Receiver on PLAT-I . . . . .	45
4.2.2	The effect of echosounders on the Gemini 720is . . . . .	46

4.2.3	Echosounders and hydrophones . . . . .	46
4.2.4	Sound projector and other anthropogenic sources . . . . .	48
4.2.5	Concurrent Operation of Gemini 720is and Aris . . . . .	50
<b>5</b>	<b>Soundscape, the turbine platform and porpoises</b>	<b>50</b>
5.1	Hydrophone measurements using the pad-float . . . . .	50
5.2	Compass performance on PLAT-I . . . . .	53
5.3	PSD from the pad-float hydrophone measurements . . . . .	53
5.4	Environmental Effects Monitoring Hydrophone on PLAT-I . . . . .	55
5.4.1	PSD of the Environmental Effects Monitoring Hydrophone on PLAT-I	57
5.4.2	Detections of Harbour Porpoise Vocalizations . . . . .	59
<b>6</b>	<b>Summary Points</b>	<b>62</b>
<b>7</b>	<b>Comments on Monitoring to Assess Risk</b>	<b>64</b>
<b>8</b>	<b>Acknowledgments</b>	<b>65</b>

# 1 Executive Summary

Sensor Testing Research for Environmental Effects Monitoring (STREEM) was undertaken with Sustainable Marine Energy (SME) and Luna Ocean in October and November 2018. Early tests of imaging sonar were made using a drifter-target system in St. Mary's Bay with sonar and other equipment operated from a small research vessel. Subsequently, the project shifted operations into Grand Passage and focused on mounting sensors to SME's PLAT-I, a floating in-stream turbine platform, so that sensors could be tested and protocols developed in order to achieve effective environmental monitoring.

The ultimate objective of such environmental monitoring is to quantify the risk that in-stream turbines pose to marine animals. To that end, we are concerned with evaluating the performance of imaging sonar for detecting and tracking animals from far upstream and then using optical cameras to identify animals that approach close to a turbine and to observe animals very near a turbine. Such a measurement system has the potential to evaluate both the number of animals that approach turbines from far upstream and the extent to which such animals avoid the area swept by the turbine rotors.

PLAT-I is a large trimaran with a central hull extending far forward of the starboard and port hulls. The port/starboard hulls and the bridge that joins them to the main hull are well situated for mounting environmental sensors to monitor marine animals from upstream until the turbines that are attached across the stern. Being far forward, the bow of the central hull served as a convenient launch point for targets that were used to test the performance of imaging sonar and optical cameras as targets drifted with the current, towards the stern.

The Gemini 720is imaging sonar reliably detected, and tracked, targets over a wide area upstream. The length of small, fish-size targets might be roughly estimated when the target is sufficiently close but shape was too poorly resolved for identification. The Aris imaging sonar gave higher resolution images (still insufficient for identification) whenever the target entered within its more limited field of view. Both imaging sonars resolve a range and an angle but integrate targets over the other dimension. Tests indicated that all three dimensions might be measured, for a small field of view, by using both imaging sonars. Gemini resolving range and azimuth in the horizontal and the Aris rotated to resolve range and the vertical dimension.

Optical cameras serve much better for animal identification in the relatively clear and well lit waters of Grand Passage. Rapid biofouling requires that the windows of camera housings be frequently cleaned in order to get reasonable images out to a range comparable to the scale of the turbine. Effective environmental monitoring would be facilitated by mount systems that enable camera equipment to be recovered for servicing and cleaning at any stage of the tide.

Preliminary results indicate that a combination of optical cameras and imaging sonars might serve to place some bounds upon the risk that in-stream turbines may pose to fish. Our measurements demonstrate, however, that careful attention must be given to how instruments are mounted and oriented in order to avoid spurious signals caused by reflections from parts of PLAT-I and its mooring system. Importantly, the instrument mount system must be capable of placing instruments near the depth of the turbine (axis of rotation at 5 m) in order to optimize the field of view and avoid near surface bubbles.

Interoperability of active and passive acoustic instruments was tested. Joint operation of sonar and high-resolution tracking of acoustically-tagged fish seems feasible. The Gemini imaging sonar was adversely affected by the research vessel's echosounder/fish finder. Hy-

drophone measurements show that the both imaging sonar and the echosounder/fish finder cause sound that some marine mammals may be sensitive to. Thus, passive acoustic methods are preferred for detecting and locating vocalizing marine animals and such measurements are best made in conjunction with optical cameras but perhaps without sonar operating.

Interoperability tests indicated that Vemco HR2 receivers functioned well with a nearby Gemini sonar. Furthermore, a HR2 receiver mounted to PLAT-I reliably detected acoustic tags nearby. The 180 kHz PPM signal from a Vemco tag sometimes caused spurious signals in measurements by Gemini sonar, but these spurious signals had a clear and distinctive structure which makes them easy to recognize and discard.

## 2 Introduction

Large-scale human civilization with heavy reliance upon fossil fuels has been associated with undesirable environmental changes and may not be sustainable over the long term [1, 2, 3, 4]. Attention has turned, therefore, to the possibility of replacing fossil fuels with renewable energy. Presently, hydroelectric dams are the largest source of renewable electric energy [5] but they are associated with ecological impacts [6, 7, 8]. Similarly, low-head tidal impoundments have been demonstrated effective for generating electricity but have been associated with fish mortality [9].

In principle, a great deal of renewable energy can be obtained by deploying in-stream tidal turbines in the Bay of Fundy [10]. There are reasons to expect that the environmental impacts of in-stream turbines will be far less than hydroelectric dams and low-head tidal impoundments. First, in-stream turbines operate in open water so pressure forces are relatively small. Second, marine animals might avoid an in-stream turbine because their path is not constrained by a dam (or tidal barrage).

To test the efficacy of in-stream turbines, the Fundy Ocean Research Centre for Energy (FORCE) has established a Test Site in Minas Passage, Bay of Fundy. Much baseline knowledge has been obtained regarding tidal currents, ambient sound and marine animals in Minas Passage and at the FORCE Test Site [10, 11, 12, 13, 14, 15, 16].

Regarding tidal power development in Canada, **the question** for which legislation [17] requires an answer is:

*Will marine animals be harmed in some way when they encounter a turbine?*

To address the question, regulators require that tidal power developers undertake “Environmental Effects Monitoring” (EEM).

In-stream turbine deployments at the FORCE Test Site have included EEM. Difficulties were experienced with both turbine testing and EEM [18]. Presently, it is not known whether or not marine animals will be harmed when they encounter an in-stream tidal turbine at the FORCE Test Site. All that can be said is that encounters should be expected [19].

The purpose of the present project is Sensor Testing Research for Environmental Effects Monitoring (STREEM). Thus, we take a step back from the immediate constraints of an Environmental Effects Monitoring Plan (EEMP) in order to evaluate equipment and methods for more effective Environmental Effects Monitoring.

For EEM that might answer the question, tidal power developers in the Bay of Fundy presently have several measurement methods at their disposal:

- Passive acoustic monitoring (PAM): Hydrophones to detect vocalizing animals [14], acoustically-tagged animals [11, 12], ambient sound, and sounds from the turbine installation [20].
- Active acoustic monitoring (AAM): Imaging sonar to detect and obtain some positional information on marine animals approaching the turbine [21, 22].
- Optical cameras (video) to detect marine animals very near the turbine [23].
- Direct visual observations.

Sustainable Marine Energy’s plan to bring their PLAT-I turbine installation (Figure 1) to Grand Passage in late summer 2018 presented an opportunity for testing the utility of the above methods for “environmental effects monitoring”.

As a research platform, the installation of PLAT-I at Grand Passage was expected to be advantageous relative to working from a gravity-base turbine installation at the FORCE Test Site: (1) Slower currents in Grand Passage were expected to make it easier to test ideas that might ultimately be translated to Minas Passage. (2) Optical methods became practicable, given the relatively clear water at Grand Passage and near-surface turbine operations during daylight hours. (3) PLAT-I seemed accessible for adaptive experiments to develop environmental effects monitoring methods and to test and service monitoring equipment.

The goal of the STREEM project was to test the utility of AAM, PAM and optical video for “environmental effects monitoring”. Given previous experience [18], evaluating effects of active acoustic devices on passive acoustic measurements was of particular interest.

It was also deemed important to evaluate performance of both AAM and PAM under idealized conditions. Thus, drifter-target experiments were undertaken to evaluate target detection by imaging sonar. This method allows for more controlled measurements under less turbulent conditions and avoids the limitations caused by the shallow water at the PLAT-I mooring location in Grand Passage. This method was also favourable for measuring instrument interactions.

Effective use of multiple technologies was another focus. By effective use, we mean obtaining measurements and methods that can be analyzed in a fashion that is both accurate and complete. Accuracy and completeness are never fully achieved, so using multiple technologies to obtain multiple lines of evidence serves to bolster confidence.

The dangers of incomplete analyses of a single type of evidence can be seen in a study by Broadhurst et al., (2014) [24] which used a video camera to monitor a commercial-scale in-stream turbine. That study [24] reported no observations of fish encountering the moving turbine. The result was, however, questionable. Broadhurst et al., (2014) examined only 5 frames that were randomly selected from the first 2 minutes of every hour.

Redden and Sanderson (2016) [19] estimated plausible encounter rates for striped bass and sturgeon with turbines at the FORCE Test Site. Those encounter rates were low, therefore subsampling video records is insufficient to draw conclusions about fish-turbine interactions.



Figure 1: Wide-angle view of Sustainable Marine Energy’s (SME’s) PLAT-I looking sternwards from the bow. Photographs and image stitching by Mike Adams.

A complete analysis of the video record would be a minimal requirement for even a rough estimate of collision/strike events. Furthermore, the field of view for an optical camera is small compared to the distance at which echosounder measurements suggest that fish exhibit avoidance [25]. Fish avoidance behaviour has also been observed nearer a turbine using high-resolution imaging sonar [26]. By mounting two sonar systems as well as optical cameras to PLAT-I, *STREEM* explored the idea of tracking marine animals over an area that extends from far upstream to the turbine.

### 3 Target detection by imaging sonar and camera

Efficacy of target detection was measured in two ways. First the boat-mounted Gemini 720is sonar was used to detect known targets that were suspended beneath a drifter in St. Mary's Bay. These were intended to test the sensor in relatively deep water under calm conditions with slow currents and low turbulence. The second set of measurements were undertaken with the Gemini 720is mounted to PLAT-I in order to measure targets drifting from upstream with the fast tidal current. It is anticipated that the first measurements might inform target detection from PLAT-I and aid with the interpretation of any change in sonar performance that might be associated with fast & turbulent currents, the more shallow water in Grand Passage, and interference with PLAT-I structures. Tests were also undertaken with an optical camera mounted with the Gemini 720is and an Aris sonar mounted nearby. Testing this combination of instruments is intended to demonstrate the possibility of tracking targets from well upstream to the location of a turning turbine — with results from the far-field sensor (Gemini 720is) informing the analysis of near-field sensors (Aris sonar and optical video camera).

#### 3.1 Boat mounted imaging sonar and target-drifter

Test targets (fish and non-biological items) were suspended beneath a target-drifter that was designed to hold targets at a known depth, known orientation and known position. Figure 2 shows a schematic of the drifter and a photograph when deployed on 19 October 2018. The target-drifter had a long, horizontal surface float with two 3/16 braided lines extending to a rebar spreader-weight at depth. GPS with compass (Aaronia) gave the position and orientation of the float (and rebar). A cross-line was attached at either 5 m or 10 m below the sea surface. Targets were tied to this cross-line, thereby being held at known depth, position and orientation. The cross-line was shorter than the rebar (and float) so that tension stretched it horizontally. A GOPRO camera was mounted to face downwards from the surface float, thereby validating targets and providing a check should non-target sub-surface animals/objects swim/drift into the target area.

The Gemini 720is imaging sonar was pole-mounted near the stern on the starboard side of the research vessel (RV Puffin) and positioned 4 m below the sea surface. The top edge of the Gemini beam was horizontal to the sea surface, with the lower edge pointing 20 degrees downwards. With respect to the azimuth, the Gemini was directed astern with the beam spreading 60 degrees to each side. Measurements by boat-mounted instruments were made on two days — 13 and 19 October.

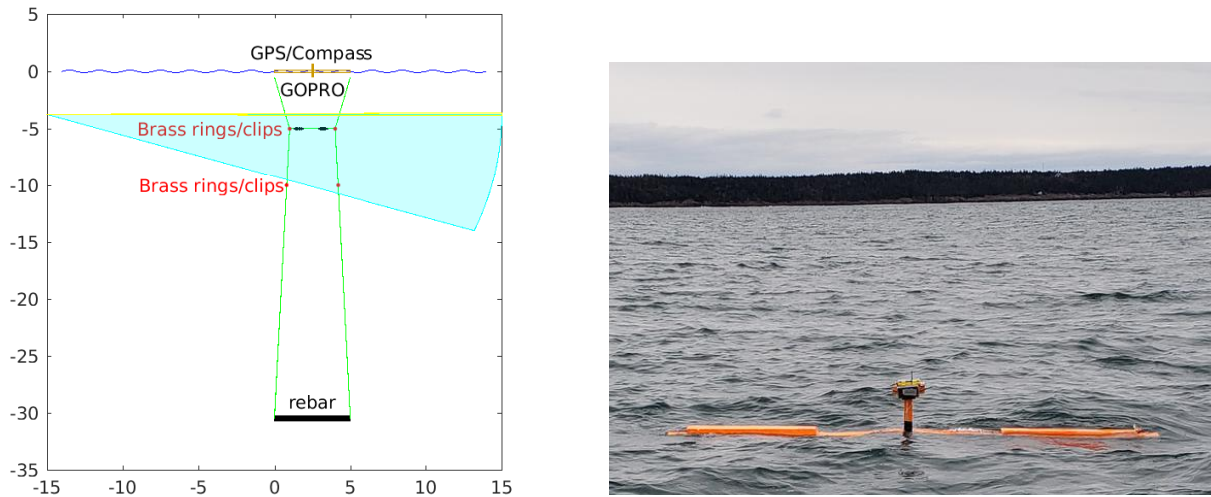


Figure 2: LEFT: Schematic of the *target-drifter* with two targets. Vertical spreading of the Gemini beam is shown with cyan. Horizontal resolution of the Gemini (twice the 1/4 degree from one beam to the next) is shown with yellow. RIGHT: Deployed target-drifter during a brief period of calm. Photo credit: Mike Adams.

### 3.1.1 13 October 2018

Experimental protocol for boat-mounted sensors called for calm conditions but such conditions were rare in October. A decision was made to undertake an initial set of measurements under “less than optimal conditions”. Winds were from the NW and W, so there was a degree of shelter on the eastern side of St. Mary’s Bay. Weather conditions worsened (wind strengthened with white caps evident and light rain) and the experiment was terminated after a 1.25 hour period of measurements.

The original measurement protocol called for rowing RV Puffin when making measurements. In calm conditions this allows the vessel to be accurately oriented orthogonal to the targets (or at any other angle of interest) and slowly rowed away, and back; all with minimal water disturbance. Given the wind conditions at the time, this was not possible. The method was adapted so that RV Puffin backed up to the target float under power and then drifted away with the wind, using the oars to keep the target-float astern (i.e. near the centre of the Gemini 720is beam).

The basic idea of this experiment was to test how the Gemini imaging sonar detected a variety of targets, at various orientations, ranges, and depths. From beginning to end of this preliminary experiment, the target layout was:

- A headless, gutted BC wild salmon, 40 cm long and 1.3 kg.
- A 4 litre plastic bag, filled with fresh water (convenient “reference” target).

Both of these were attached to a cross-line at 5 m below the sea surface. The cross-line was attached using brass clips (Figure 3) that fitted onto rings at the 5 m level. The original idea was that this arrangement would enable us to quickly change targets by switching out cross-lines, or to move the cross-line down to rings at 10 m depth.

The speed of sound is very much faster in brass (and other metals) than in water. Additionally, metals are much more dense than water. Thus, the acoustic impedance of the brass



Figure 3: Shackle and brass clip: Brass clips were used on the cross-line for the target float on 13 October 2018. The shackle was used to weight targets that were cast from PLAT-I on 23 October 2018. Photo credit: Connor Sanderson.

ring/clips is much greater than for water and so there is a signal returned from each Gemini transmission. Figure 4 shows that these small metallic parts of the drifter assembly show up on the imaging sonar. Scintillation causes considerable variation in the amplitude of the signal returned from each target, and that variation changed from one image frame to the next. Also, especially at greater range, scintillation causes the image-position of a target to jitter, from pixel to pixel. With hindsight, we therefore regard the clips and rings as being more nuisance than convenience.

At closer range, with Gemini 720is sonar gain set to 100%, the reference target (4 litre plastic bag filled with fresh water) shows up in the image (right inset of Figure 5) as an intense return that is smeared across the azimuth,  $\theta$ . This is a natural consequence of the physics behind a multi-beam sonar. The mathematical description of this physics is analogous to that of  $N$ -slit diffraction. Return intensity will be

$$I = I_0 \left[ \text{sinc} \left( \frac{\pi a}{\lambda} \sin \theta \right) \right]^2 \left[ \frac{\sin \left( \frac{N\pi d}{\lambda} \sin \theta \right)}{\sin \left( \frac{\pi d}{\lambda} \sin \theta \right)} \right]^2 \quad (1)$$

where  $a$  is slit width,  $d$  is separation between slits, and  $\lambda$  is wavelength. This equation gives a strong return at the angle of interest with numerous smaller wiggles off to the side (side lobes). The strong signal in the middle is the target. The side lobes are false representations of the target. One method for removing the side lobes is to set a threshold level that will clip lower amplitude side lobes. Obviously, when there is a very strong target the threshold might need to be adjusted so high that other desired targets are removed along with the side lobes. We have communicated with the manufacturer to suggest a method for processing instrument measurements in a way that should minimize this issue and actually exploits the side lobes to get a clean signal. Presently, a Gemini 720is user does not have access to the part of the data stream required to test/apply the method.

The left inset of Figure 5 shows that the angular spreading is not an issue when the Gemini

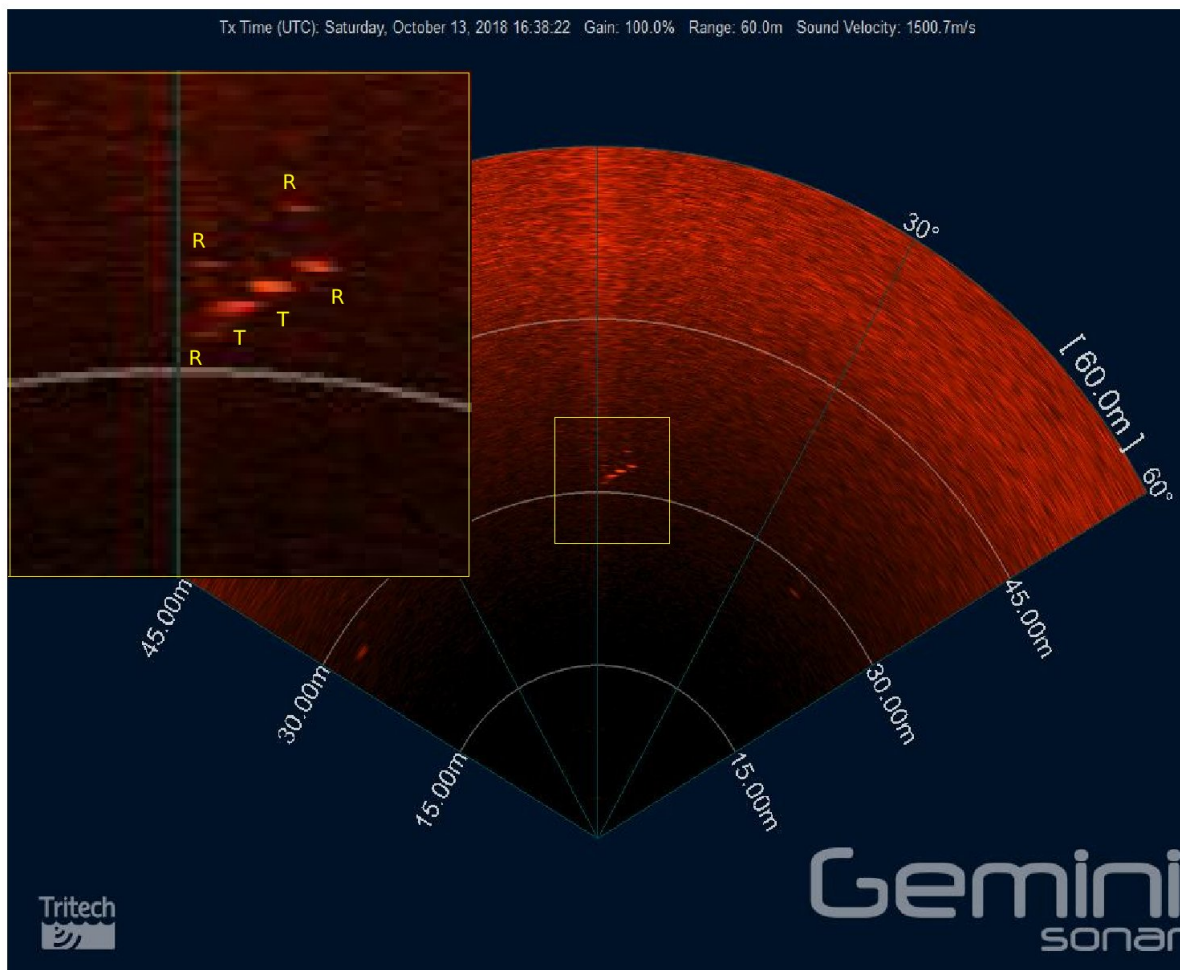


Figure 4: Gemini 720is sonar image, taken 1638:22 UTC 13 October 2018 with 100% gain. The T denotes two targets (reference and salmon) at depth 5 m below the sea surface. Signals from the ring plus clip are denoted R, beside the targets. Signals from deeper rings appear a little further away.

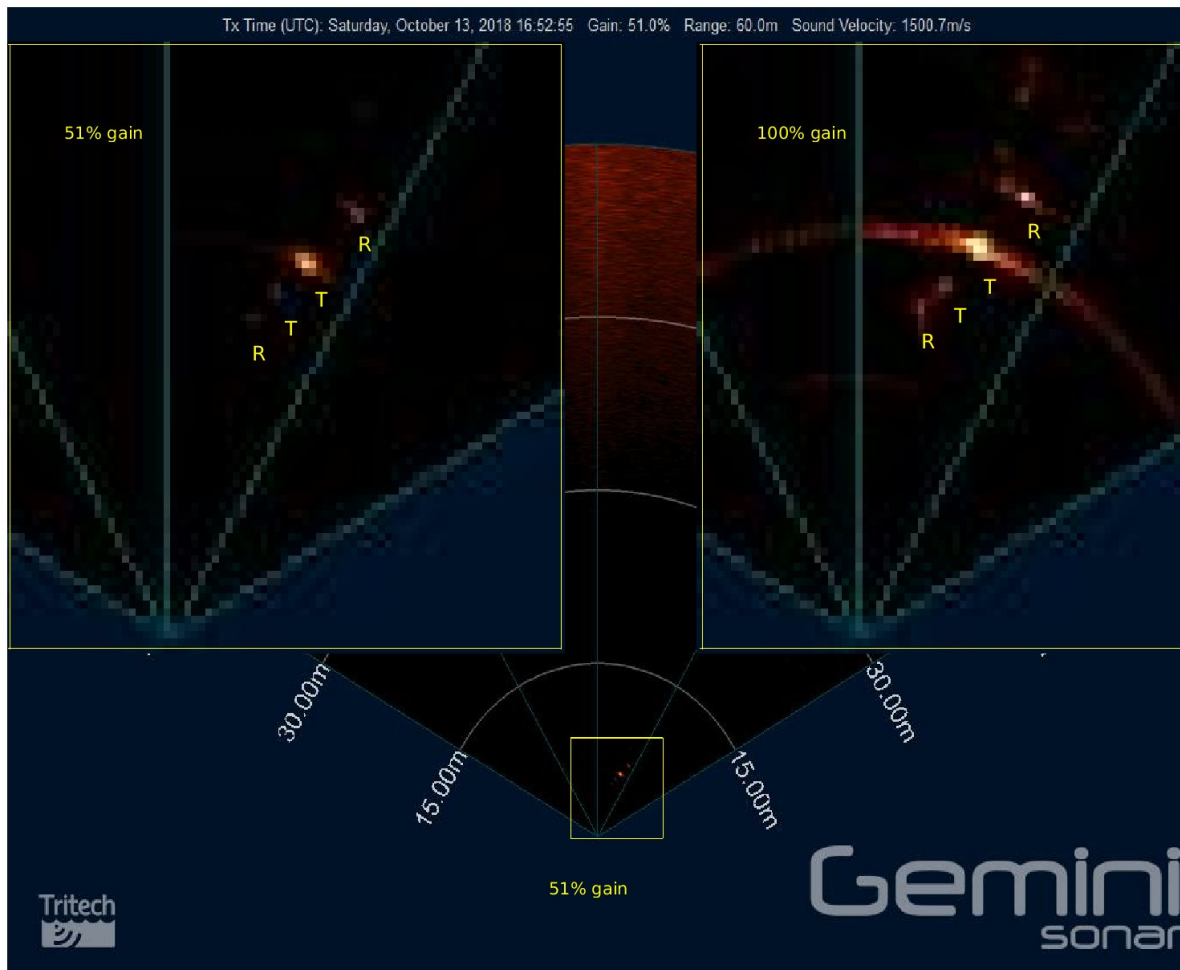


Figure 5: Gemini 720is sonar image, taken 1652:55 UTC 13 October 2018. The main image is taken with 51% gain and the left inset shows a zoomed in view. The right inset shows a zoomed-in view about a second later when the gain had been increased to 100%.

gain is dialed back to 51%. Essentially, this reduces the amplitude of the recorded signal<sup>1</sup> so that the side lobes fall below the threshold level. An obvious disadvantage of this strategy is that weakly reflecting targets will also disappear below the threshold.

It should be noted that the shape of the salmon target could not be discerned, even at close range (about 7 m in Figure 5). The Gemini 720is has 512 beams spanning 120° which corresponds to a pixel size of  $\approx 0.25^\circ$  and angular resolution  $\approx 0.5^\circ$  (Nyquist Sampling Theorem). At 7 m range, an angular resolution of  $0.5^\circ$  corresponds to 6 cm resolution. Perhaps we might have anticipated the salmon to appear as a highly pixelated image. Admittedly, the maximum range was set to 60 m so the Gemini display software may also limit resolution. Generally, the Gemini imaging sonar is best used to scan for targets over a wide field of view and to track them over some distance. While detecting and tracking targets over a large region is very useful, it is probably asking too much to require a sonar set up in this way to also be useful for target identification. Of course, very large targets (e.g., marine mammals) would show some sort of identifiable shape. Sometimes sonar images show the same shape that one obtains using an optical camera [27], but not usually. Large animals are less common than small animals [28] and some of them might be averse to sonar [29], so large animals are less likely to appear in sonar images.

Ideally, to test resolution of target shape, we would obtain measurements with: (a) the target very close by, (b) maximum range setting not too much greater than range to the target, (c) the target oriented with length spanning the angular dimension. Such an image is shown in Figure 6. Unsurprisingly, the reference target is returning a very strong signal and has side lobes distributed across the angular dimension. The length and orientation of the salmon is apparent, although shape is not and it would take a leap of faith to say which was the tail end.

It is pertinent to compare the Gemini detection of a 40 cm salmon (Figure 6) with an optical image at similar resolution. To do this, we begin with an image of a 20 cm salt herring (headed and gutted) that was obtained on 23 October using a GOPRO camera mounted to PLAT-I when the herring was at about 3.3 m range (Figure 7). Averaging this image to  $0.25^\circ$  pixels gives the image shown in the right panel of Figure 7. The salmon is twice the length but also twice as far away. Thus, it is fair to compare the salmon signal in Figure 6 with the pixelated signal in the right panel of Figure 7. The length and orientation of the herring (headed and gutted) is apparent and shape is poorly represented.

### 3.1.2 19 October 2018

Given uncertain weather and experience gained from the 13 October experiment, it was necessary to adapt the experimental method in several ways:

- The brass clips and rings were removed from the target-drifter (Figure 2). Rings were replaced by loops in the vertical-lines and thin plastic cable ties used instead of the brass clips.
- Working in more windy conditions required working closer to the lee shore, where water depths may be reduced. Thus, vertical-lines of the target-drifter (Figure 2) were shortened from 30 m to 20 m. This raised the level of the rebar bottom-weight which

---

<sup>1</sup>Gain setting does not change the transmitted signal, nor the return signal. It just changes the extent to which the return signal is amplified for display and storage.

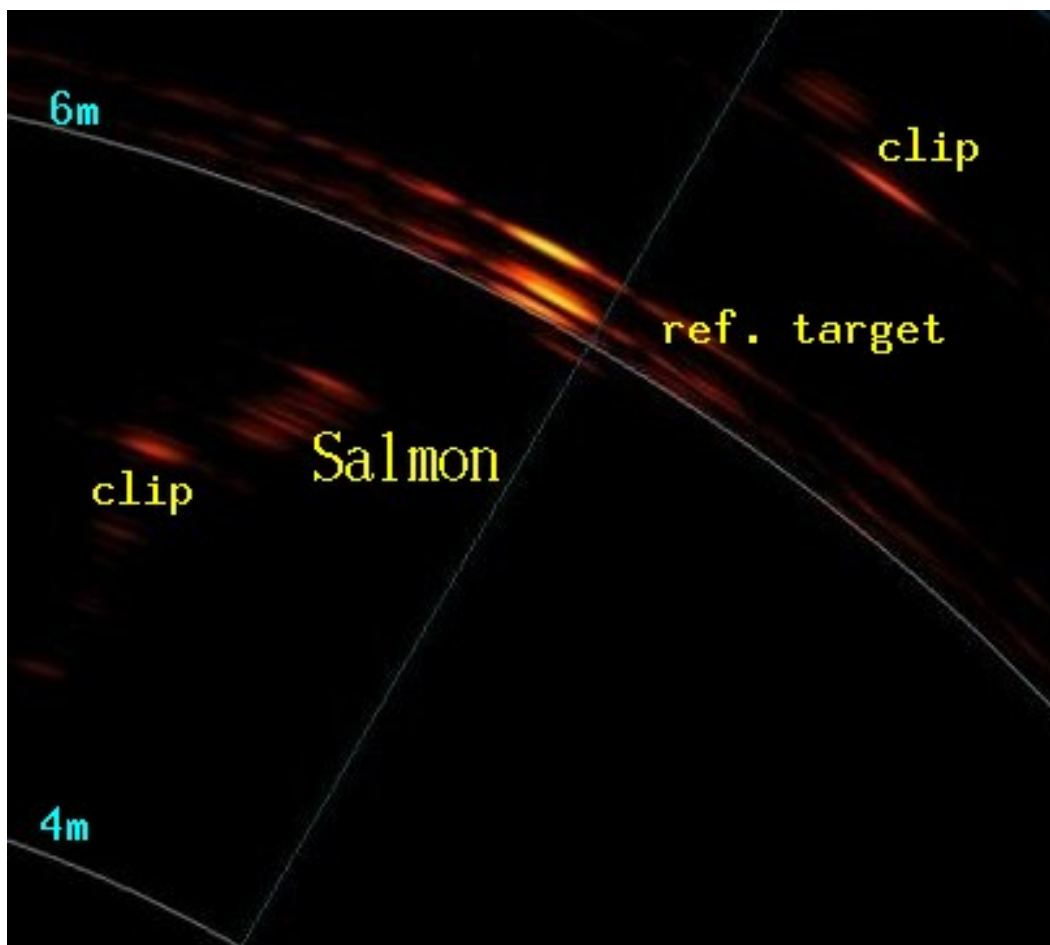


Figure 6: Gemini 720is sonar image, taken 1643:17 UTC 13 October 2018 with gain set to 100% and maximum range set to 7.5 m.

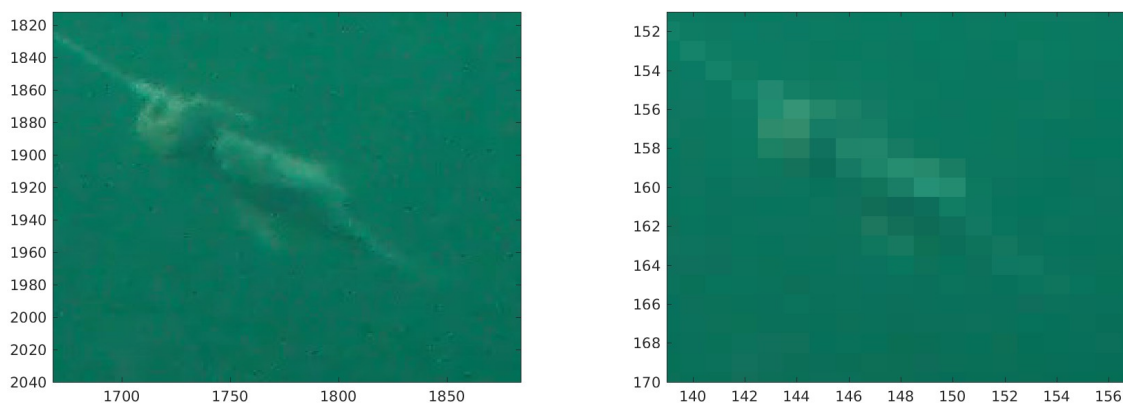


Figure 7: LEFT: GOPRO image of a 20 cm herring at 3.3 m range. RIGHT: Pixel size averaged to  $0.25^\circ$ .

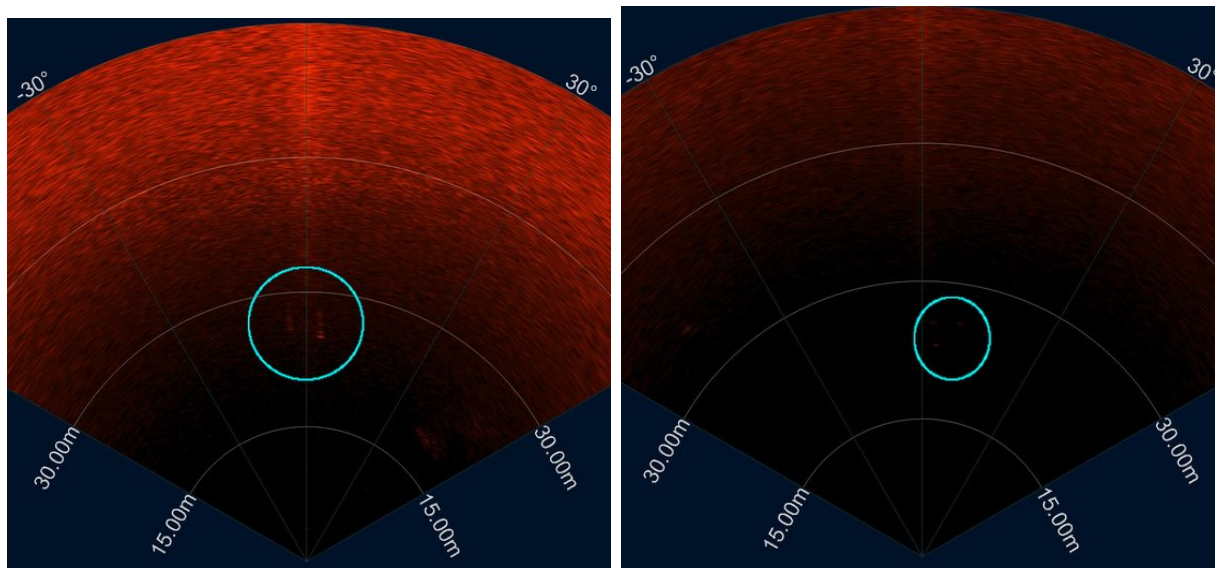


Figure 8: Control experiment: target-drifter without targets. LEFT: The vertical lines return a weak shadow when the gain is 100%. RIGHT: Tiny, weak, point-like, signals might be present when gain is 50%.

limited the range at which reliable measurements could be made, especially when the boat pitched in rough conditions.

- Two synchronized icListenHF hydrophones (Ocean Sonics Ltd) were incorporated as targets. Thus, any effect of the Gemini 720is sonar on passive acoustic measurements (hydrophones) could be quantified, see §4. A Vemco High Resolution (HR) acoustic fish tag was also added, between the hydrophones, so that the synchronization could be confirmed. Given the addition of the HR tag, we also hung a HR2 receiver from the port side of the stern in order to test interoperability of HR Vemco technology with the Gemini 720is sonar. Results from this part of the experiment are reported in §4.1.5.

Again, measurements were made by using the oars to steer the boat while the wind blew it away from the target-drifter. An html document [30] was prepared that includes hyperlinks to Gemini 720is data obtained during each drift. Thus results have been sorted and documented so they can be conveniently viewed in movie form, providing Gemini display software is installed. Presently, we will show only a few frames from those movies, corresponding to when the Gemini 720is was about 25 m from the target — similar to the maximum practicable range that might be achieved in the shallow waters of Grand Passage where the PLAT-I has been moored.

A control experiment was undertaken, with no targets attached to the target-drifter (Figure 8). The vertical-lines show up as weak lines running radially when gain is set to 100%. With gain lowered to 50%, the vertical-lines were not apparent but the loops and cable ties used to attach the cross-line seemed to present as small dots that are difficult to see. Vertical lines are made from 4 mm diameter braided nylon. It would be better to use thinner lines. However, given unfavourable Fall weather conditions, it was judged prudent to ensure equipment durability at the expense of some compromise in the quality of measurements.

Drift tests were made using synchronized hydrophones and the Vemco HR tag at two

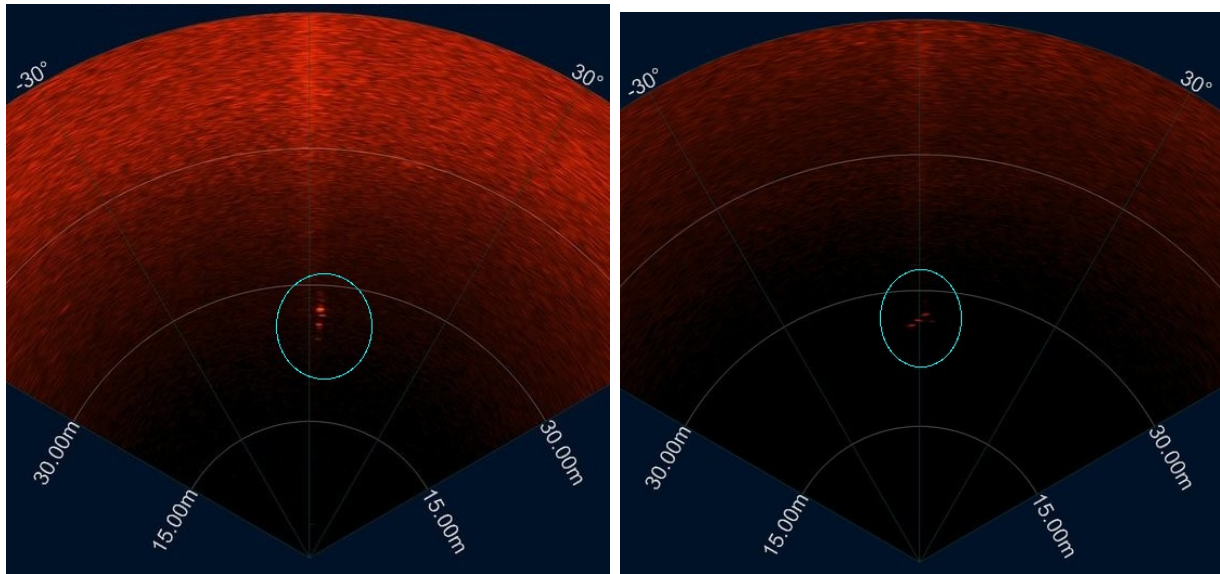


Figure 9: Gemini images of two hydrophones and a Vemco tag (not transmitting) when the cross-line is 10 m below sea surface. LEFT: Gemini gain is 100% and the target is aligned along the beam. RIGHT: Gemini gain is 50% and the target has more of a cross-beam alignment.

depths: 5 m and 10 m below sea surface. In each case, multiple drifts were made to test results with Gemini gain set to: 100%, 50% and 10%. For each drift, we also operated the HR2 receiver from the stern on the port side (results reported in §4.1.5). Figure 9 shows images when hydrophones and Vemco HR tag were at 10 m below the sea surface and the Gemini was at a range of about 25 m. With 100% gain (LEFT panel) the hydrophones are evident but the signal is somewhat confused because the target is oriented along the direction of beam propagation so the vertical lines are juxtaposed and there may be shadowing effects by the closest hydrophone. The RIGHT panel shows results when gain is 50% and the target is oriented more in the azimuth. Now the vertical lines are not evident and three targets are more clearly seen: the two hydrophones plus the Vemco HR tag. Note, the Vemco HR tag was not transmitting at the time of the image (see Experiment 4 for when it did) but it is tuned to resonate at 180 kHz and clearly also responds strongly at the 720 kHz frequency of the Gemini 720is. This is not surprising, given that 720 kHz is a harmonic of 180 kHz. This raises a *possibility* that the Gemini might be able to identify tagged fish among other fish that are not tagged.

Similar measurements were made using a macroalgae target along with the reference target on a cross-line at 5 m below sea surface (Figure 10). It should be noted that background noise is displayed more prominently as range increases. This is to be expected, since total scattering increases with path length and also because vertical spreading of the beam is more likely to result in reflections from the seafloor or sea surface when range is large. When gain is dialed down, the background signal remains below threshold out to a greater range. Both the macroalgae and the reference target returned strong signals. The macroalgae was freshly harvested from the rocks in Grand Passage, so gas vacuoles probably explain the strong signal return. Macroalgae is commonly seen floating in Grand Passage, mostly near the surface, and tends to wrap around poles used to mount instruments from PLAT-I. We sometimes observed very small pieces of degraded macroalgae in the optical images taken 2 or more metres below

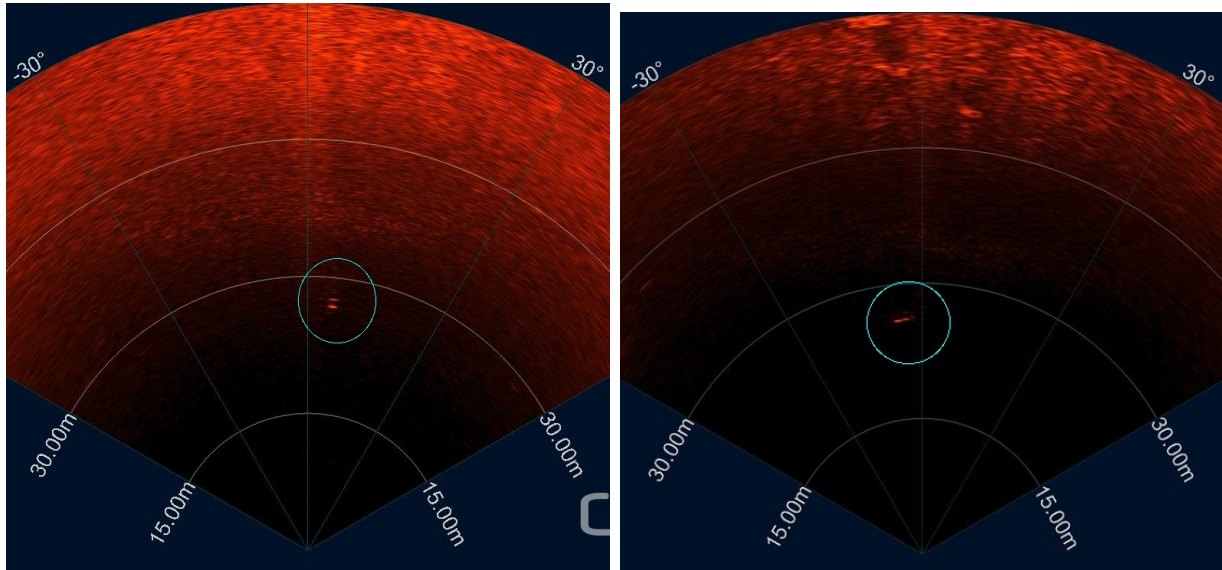


Figure 10: Gemini images of the reference target and macroalgae when the cross-line is 5 m below sea surface. LEFT: Gemini gain is 100% and the target is aligned along the beam. RIGHT: Gemini gain is 50% and the target has more of a cross-beam alignment.

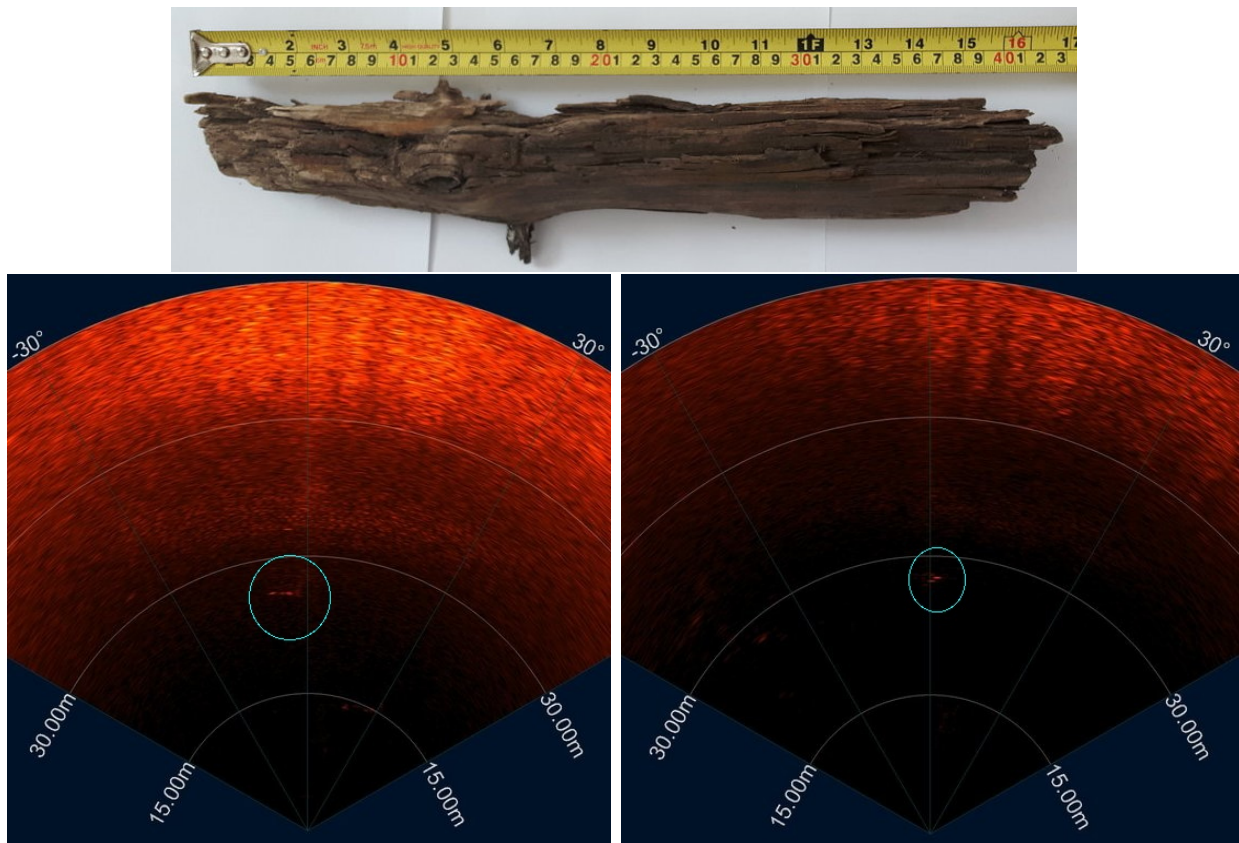


Figure 11: TOP: Photograph of water-logged wood (42 cm × 6 cm). Lower panels show Gemini images of the reference target (4 L plastic bag filled with fresh water) and water-logged wood (TOP) when the cross-line is 5 m below sea surface. LEFT: Gemini gain is 100%. RIGHT: Gemini gain is 50%. Photo credit: Connor Sanderson.

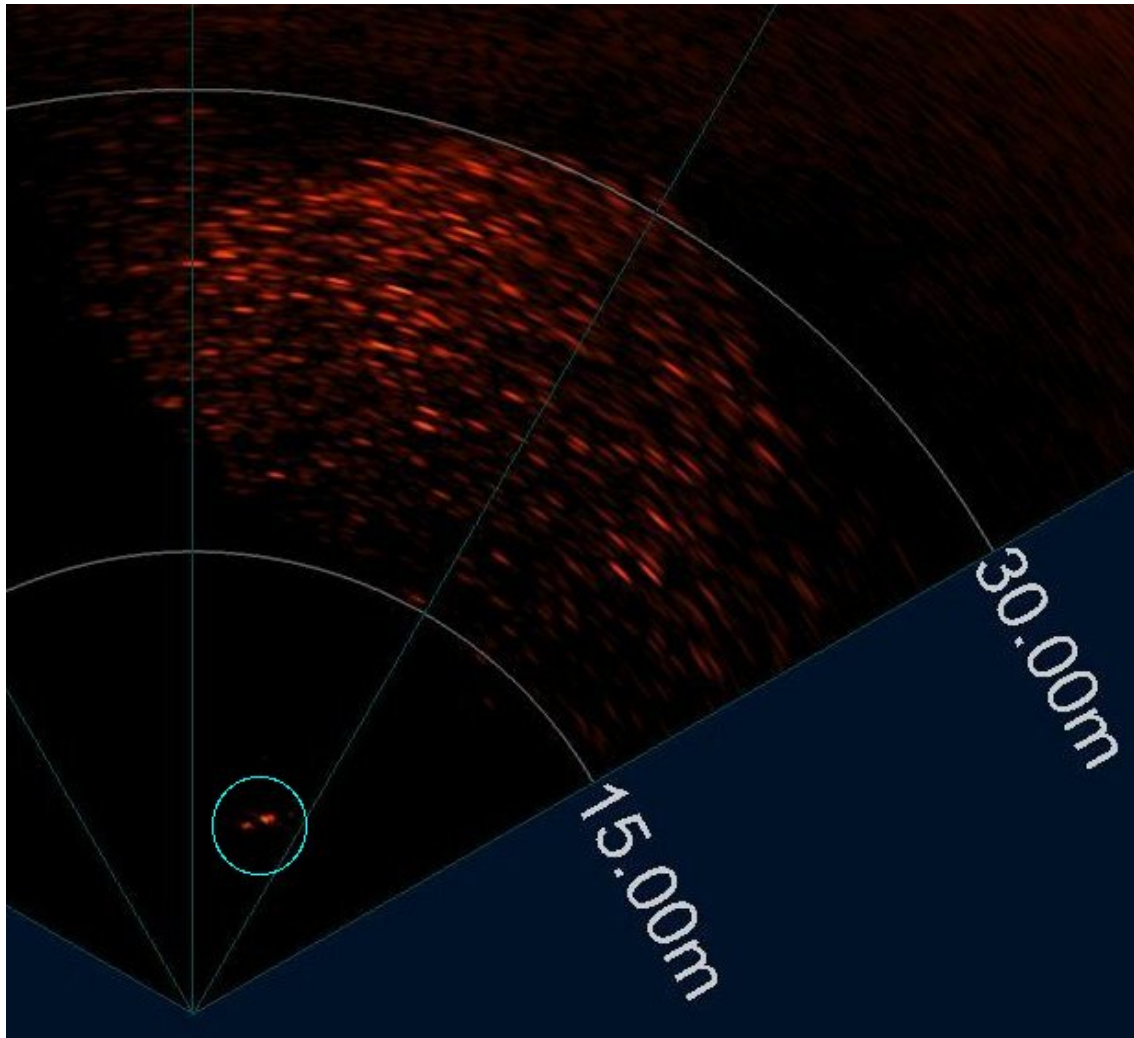


Figure 12: Gemini images of the reference target (4 L plastic bag filled with fresh water) and water-logged wood when the cross-line is 5 m below sea surface, maximum range is 60 m, and gain is 50%. The wood and reference target appear distinct at close range (inside the cyan circle). A school of fish is evident between 15 and 30 m range.

sea surface when our GOPRO camera was mounted to PLAT-I.

A 42 cm length of water-logged wood (Figure 11) was collected from near a wharf in Grand Passage. This was mounted beside the reference target at 5 m below the sea surface. Figure 11 seems to show the wood beside the reference target at about 25 m range. At these ranges, the reference target is very difficult to resolve from the wood target. Examining an image when the target was close by, Figure 12, shows the reference target and wood as distinct signals. A school of fish is also evident at 15-30 m range. None of the targets can be considered to have their shape resolved. Nothing can be said from the image about the species of fish in the school, except to note that they are not large fish. The image provides the user with no shape information that might resolve the wood from the reference target. It should also be noted that there is frame-to-frame jittering of targets, perhaps caused by scintillation.

### 3.2 Imaging sonars and optical cameras mounted to PLAT-I

A series of experiments were undertaken to detect and track targets using sensors attached to the PLAT-I. Figure 13 illustrates three views of PLAT-I and introduces labels which will be used in subsequent discussion.

In order to obtain high quality measurements it is necessary for equipment to be mounted at a depth commensurate with the turbine (which is the depth that must be measured). Importantly, sonar should be clear of the sea surface in order to minimize reflections associated with the air-water interface, surface disturbances (turbulence and bubbles) and flotsam which is frequently observed near the surface. Similar considerations apply for optical cameras. In the case of passive acoustic monitoring (hydrophones), it is even more important to be sufficiently below the sea surface, because PLAT-I/infrastructure interactions with the current create a great deal of bubble and noise contamination (right panel in Figure 14). These considerations are of fundamental importance, for both experimental science and for environmental effects monitoring programs.

In order to mount scientific instruments to PLAT-I, Sustainable Marine Energy (SME) provided 2 inch scaffold clamps on the inside edge of the starboard and port hulls of PLAT-I (Figure 14). Thus, the clamps were designed to hold a 2 inch vertical pole to which scientific instruments were to be attached. This mount system turned out to be insufficient for our experiments because:

- The pole could not support our equipment without excessive vibration.
- The pole could not extend to sufficient depth without buckling by both drag force and inertial forces resulting from vibration.
- Equipment could only be deployed and recovered at slack tide. Drag forces were almost overwhelming for two strong men on the one occasion when we attempted (and failed) to deploy and recover an unloaded mount pole when the tide was running.

A much better option would be:

- A single row of larger diameter clamps that were well clear of the water line. Or bolt-points well clear of the water line.
- Install an *additional beam* with bolt points that runs well above<sup>2</sup> the line of lower clamps/bolt-points.
- There are ample points on the existing PLAT-I I-beams to which this *additional beam* can be attached.

The original SME work order was for swivel clamps to be used at the lower level in order to facilitate instrument deployment and recovery at any stage of the tide. Swivel clamps were not installed. Swivel clamps could have allowed ready access to small instruments that are mounted a small distance below the sea surface but bubble and noise contamination would still be problematic. High quality scientific measurements required larger instruments to be mounted further below the surface in order to make measurements where they are required and

---

<sup>2</sup>Balancing moments and forces makes it clear that moving attachment points further apart in the vertical will reduce forces acting on mount-clamps and bolt-points.

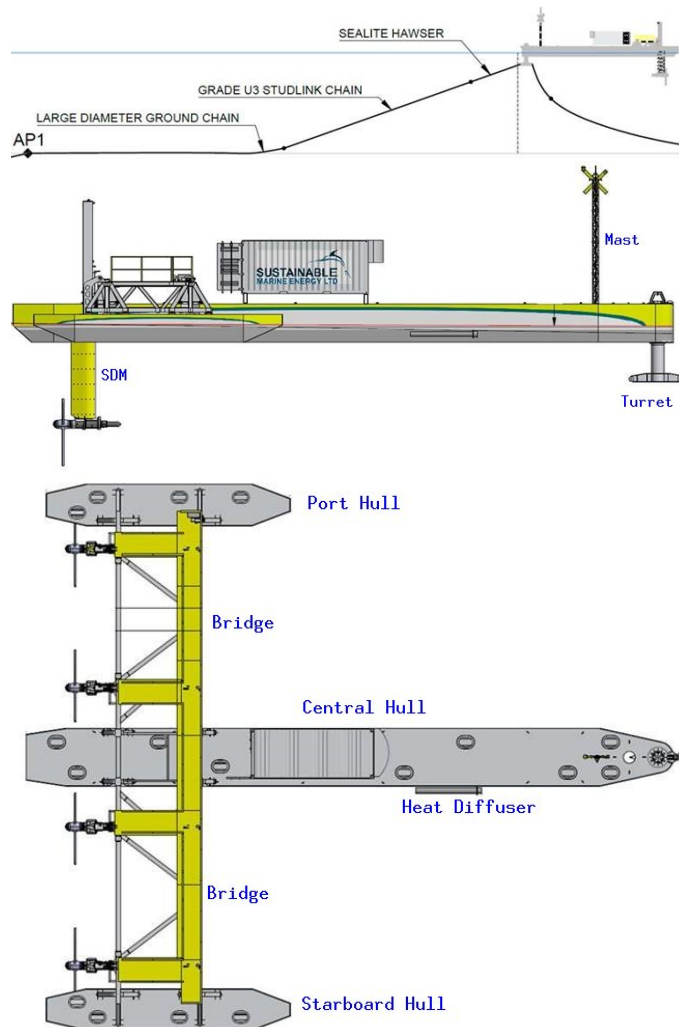


Figure 13: Illustrations of PLAT-I with labels corresponding to our discussion in the text. TOP: Mooring components. MIDDLE: Schottel Deployment Modules (SDMs) which support the turbines, FPSO mooring turret, and a mast near the bow. BOTTOM: PLAT-I has three hulls (port, starboard and central) which are connected by a bridge. Drawings provided by SME.

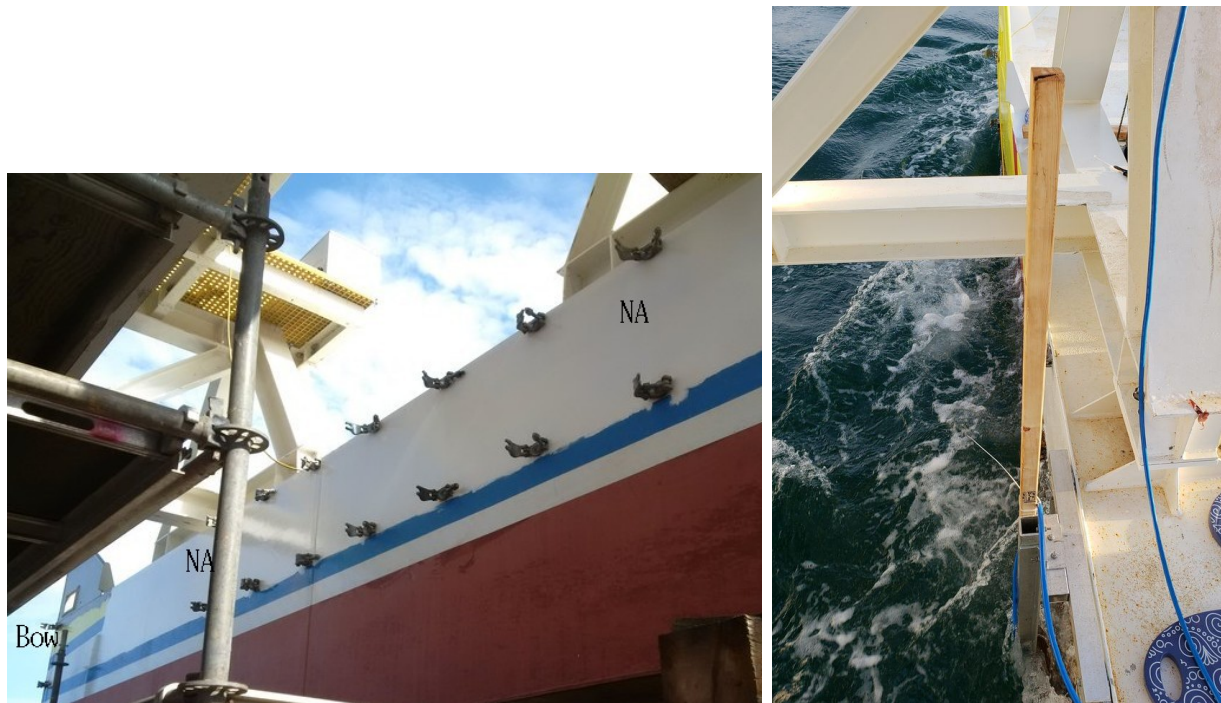


Figure 14: LEFT: The inside edge of the starboard hull while PLAT-I was being fitted out at the Metaghan shipyard. Scaffold clamps were welded to the hull in order to fasten 2 inch poles for mounting scientific instruments. Clamps marked NA were difficult to access. RIGHT: “First-generation” mount bracket and top of the “first-generation” mount pole used for the Gemini 720is. Photo credit: Mike Adams.

away from the reflecting surface and near-surface disturbances (e.g., bubbles, sound sources, and flotsam).

In order to mount scientific equipment to the existing clamps, we adopted a strategy that began by fastening a mounting bracket to the side of PLAT-I using four clamps. The mount pole could then be fastened to the mounting bracket, according to scientific requirements.

Much of our field time was spent improvising mount brackets and mount poles for the various instruments. Figure 15 shows photographs (top left and top right) of a first-generation mount system that supported a GOPRO camera and Gemini 720is sonar at 2.3 m below the sea surface. The Aris (with its remotely controlled orientation unit) was attached to the stern-most mounting bracket in the top left panel of Figure 15. Ideally, instruments should be mounted at depths close to the level of the axis of rotation of the turbines (5 m below the sea surface). The bottom photographs in Figure 15 show the second generation mounting system under construction (bottom left), and being used to deploy a Vemco HR2 receiver (bottom right).

The second-generation mounting system solved the previously mentioned problems. It had no vibrational instability, low drag, could extend to greater depth, and made it easy to deploy and recover instruments at any stage of the tide. Unfortunately, PLAT-I does not orient cleanly into the tidal currents (Figure 16). Thus, the chord of the streamlined pole often had a non-zero angle to the relative current. This generated lift forces which varied slowly as the orientation of the PLAT-I varied relative to the current. These lift forces were sufficiently strong to cause an observable flex in the mount bracket. Two solutions for the lift forces are obvious. (1) To have the streamlining swivel on the pole. (2) To hinge the pole so that it swivels on the mount bracket in which case lift forces will only act to the extent that the streamlined pole is always oriented directly into the current. The *STREEM* ended before a third-generation mount system could be applied.

### 3.2.1 Target tracking on 23 October 2018

A GOPRO video camera and two imaging sonars (Gemini 720is and Aris) were mounted to PLAT-I in order to test their utility for detecting and tracking targets. The original field plan for this experiment required four days of boat time so that float-targets<sup>3</sup> could be:

- Released upstream of PLAT-I.
- Tracked by a GPS mounted to the float target.
- Detected as they approach imaging sonars and cameras mounted to PLAT-I.
- Recovered for re-deployment.

The experiment was predicated on calm weather conditions and having no other active acoustic devices operating during this test.

Given the bubbles generated by motorized boats, and given safety restrictions on operating boats immediately upstream of PLAT-I, we improvised another method for operating the target-floats. The basic idea was to cast the target from the bow of PLAT-I, as illustrated in Figure 17. A plastic Maximum box was tied to a recovery line and used as the surface

---

<sup>3</sup>Subsurface targets suspended from a small surface float equipped with GPS.

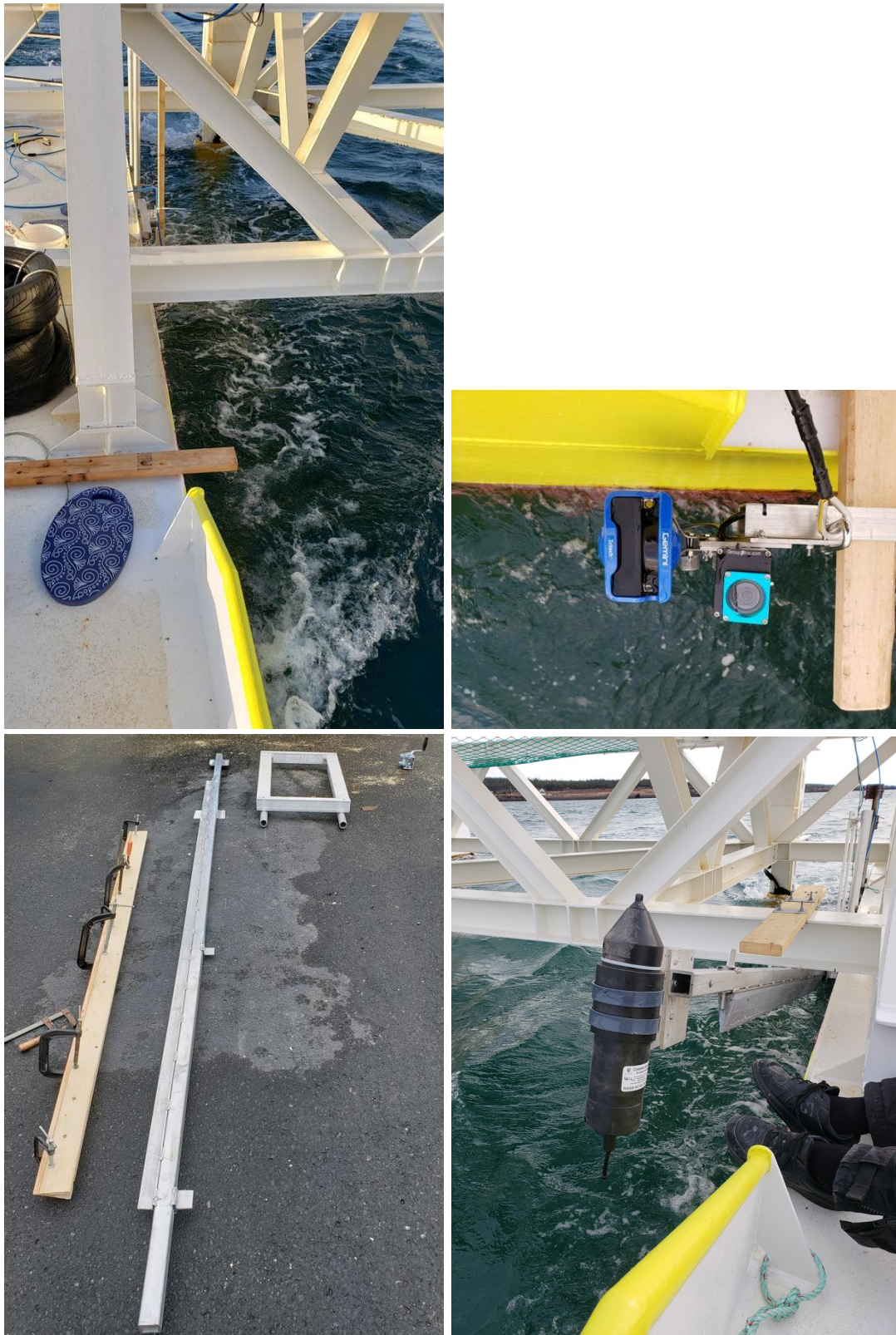


Figure 15: TOP LEFT: Looking back from the instrument recovery position to Gemini/camera and Aris “first-generation mount units” in deployed position. TOP RIGHT: Camera and Gemini fitted to the “first-generation” mount pole at the recovery position. BOTTOM LEFT: “Second-generation mount” under construction. From left to right: fairing, reinforced pole, mount bracket and winch. BOTTOM RIGHT: “Second-generation mount raised with Vemco HR2 receiver attached. Photo credit: Mike Adams.

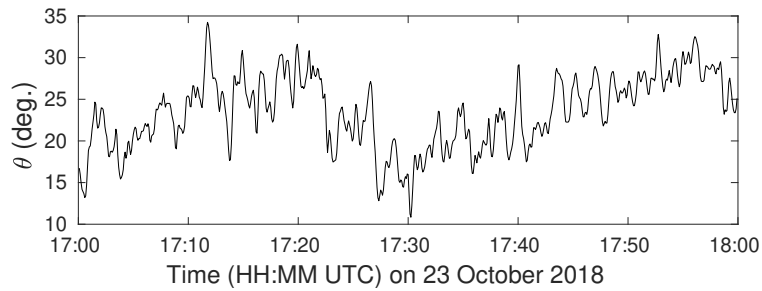


Figure 16: Fluctuations in the orientation of the bridge of PLAT-I. Measured using Garmin GPS units at each end of the bridge. GPS measurements indicated a separation distance of 24 m with standard deviation 1.2 m. Thus the standard deviation of the error in the angle  $\theta$  was  $2.9^\circ$ .

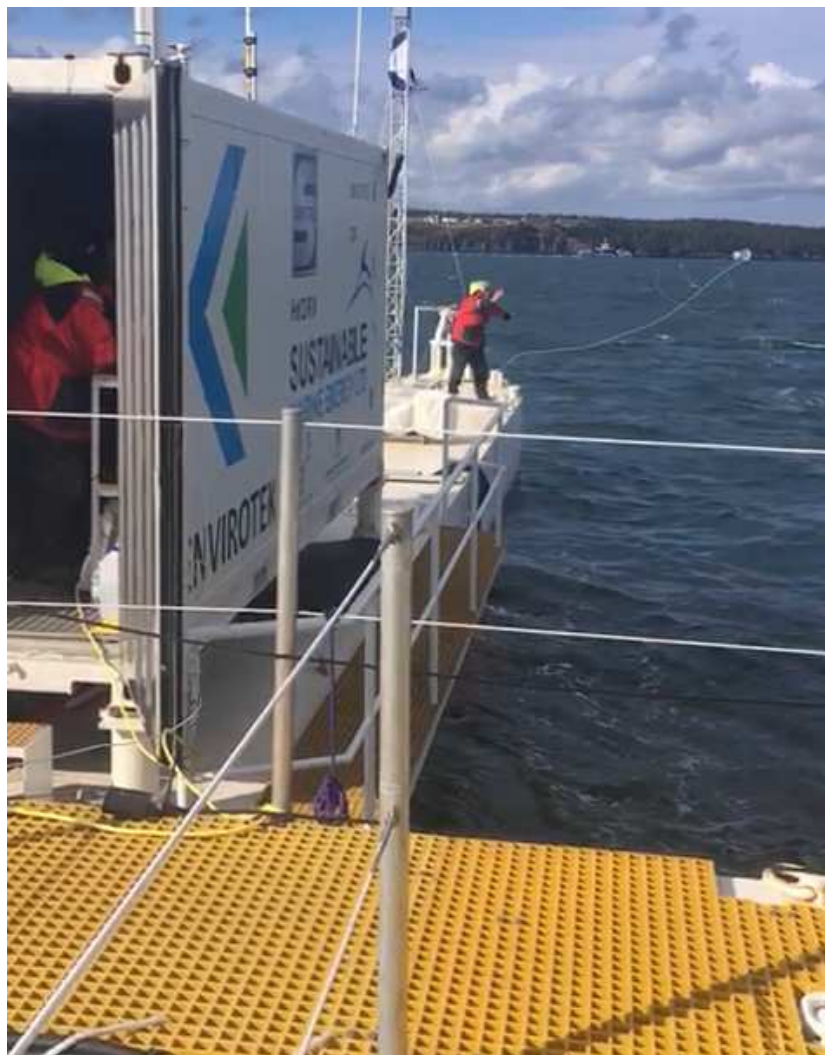


Figure 17: Casting the float-target with recovery line from the bow of PLAT-I, 23 October 2018. Photo credit: SME.

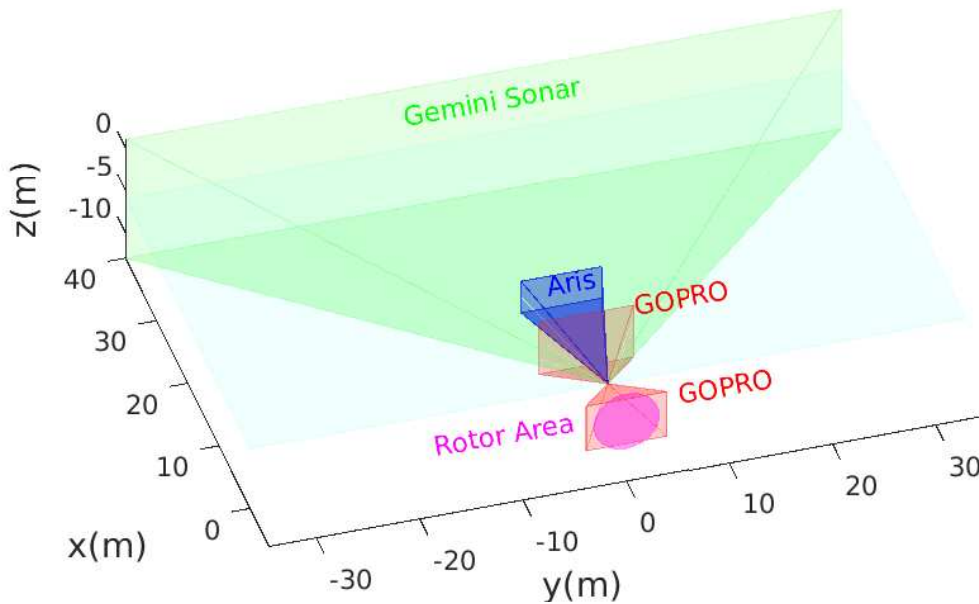


Figure 18: Generalized illustration of the fields of view for sonars and GOPRO cameras. Adaptations might be made for specific long-term monitoring objectives.

float. A shackle (Figure 3) was suspended from the surface float using 5 m of thin fishing line. Thus, the shackle was the first target that we tested. Subsequently, a 0.8 m leader was used to tether a salt herring to the shackle. The salt herring target had a total length of 20 cm. With a little practice, it was possible to cast the target so that it drifted from 20-30 m upstream and into the field of view of the optical camera. Given this level of control over the drifter trajectory, and given how reliably the Gemini 720is detected the target from the moment it entered the water, we did not need to include a GPS in the surface float.

Care was required to avoid entanglement with the heat diffuser (Figure 13) when recovering the target. The line was carefully laid out between casts in order to avoid entanglement with deck fittings. This improvised method worked well enough and has potential for generalized applications (e.g., §4.2.1) and substantial refinement. All things considered, our improvised method was both superior and more convenient than what was originally proposed.

On 23 October 2018, the first-generation improvised mounts (top panels of Figure 15) were used to measure how targets were detected by the Gemini 720is, Aris, and GOPRO camera. Figure 18 shows a schematic of the fields of view from our instrument layout. The idea, of course, is for targets to be detected over a wide area when they are far away and to be resolved with increasing detail as they approach the turbine. Turbine rotors were not installed at the time of our measurements so we did not include a camera to view the rotor. Nevertheless, we were able to demonstrate that a target could be tracked using the Gemini 720is and subsequently detected when it came within the fields of view for the Aris sonar and GOPRO video camera. A separate HTML document has been prepared [31] so that many of the measurements can be interpreted and conveniently viewed (using hyperlinks). The present discussion will be more limited in scope.

We did not see any evidence of the two sonar systems interfering with each other. On the other hand, parts of PLAT-I interfered with the performance of the Gemini 720is (Figure 19, top panel). The magenta T shows a very strong signal returned from beneath the bow of

PLAT-I. This return is caused by the “turret” (Figure 13) which is a massive steel structure that extends several meters below the bow of PLAT-I. Sonar signals returned from the turret are so strong that side lobes (1) extend across all angles at a range of about 22 m (Figure 19). These side lobes are very troublesome for that particular range but targets can still be tracked at both greater and lesser ranges. Note, however, that signals returned from the seafloor can become limiting for ranges greater than 30 m, especially at low tide. In principle, equation (1) might be used to mitigate the angular spreading caused by the turret but that requires access to low-level Gemini data, which we do not have. For many purposes, the sonar could be angled so as to avoid the turret.

Another signal is marked with a magenta C in Figure 19. This is a return from the aft anchor chain. The return is weaker when tide is strong because tension is reduced on the rear chain and it drops to a lower level. This signal becomes stronger near slack tide, but is not all that troublesome for the present instrument configuration.

The signal return labelled with a magenta D (Figure 19) is associated with the “heat diffuser” (Figure 13). The heat diffuser is used to dispose of electrical energy being generated when PLAT-I has operating turbines that are not connected to the grid. Turbines were not installed when our measurements were made. The heat diffuser created a great deal of turbulence but most of the time the Gemini signal returned from that turbulence is confined to an area near the centre hull. A strong spike causes side lobe issues near slack tide but these are confined to a very specific range that may be associated with some part of the PLAT-I infrastructure which we have not been able to identify. Near slack water, targets can be well identified from the rest of the area being monitored.

Three target detection/tracking experiments were undertaken on the ebb tide (Table 1). First, beginning at 1534 UTC, casts were made with only the shackle as a target. In this first experiment, only the Gemini and Aris were deployed. The Gemini detected and tracked every cast, as we might have hoped for given that the Gemini has a wide 120° field of view and can operate over ranges considerably greater than the upstream distance from which the target was cast. The target did not always drift within the field of view of the Aris (30° field of view over a lesser range) but when it did, the Aris detected and tracked the target reliably. Neither sonar provided images from which the target could be identified as being a shackle.

Second, starting at 1702 UTC, casts were made with a target consisting of the shackle and a short line (about 0.8 m long) that attached the salt herring. Again, only the Gemini and Aris were used for detection and tracking. Again, Gemini detected and tracked every cast of the target, and Aris detected those casts that entered within its more limited field of view. Gemini images (Figure 19) often showed the shackle and herring as separate targets, but not always, probably because the herring did not always drift clear of the shackle. On some casts, the line tangled. Aris images (Figure 19) also appeared, sometimes, to represent the shackle and herring as separate line-like targets. Neither sonar gives an image that is anything like the real shape of the target. This is as expected, given that the sonar measures one angle and a range at low resolution whereas humans see objects with two eyes that each perceive two angles at high resolution and a range at lower accuracy. Nevertheless, when sonar resolves a target at sufficient resolution it is possible to make inferences about target identity, especially when target shape and position can be tracked over a period of time.

The third experiment used shackle and herring as the target with both sonars and a GOPRO camera for target detection, tracking, and identification. The third experiment began at 1908 UTC. The casts were made with care in order to drift the target within the field of

Date	Time HH:MM UTC	Tidal height (m)
14 Oct 2018	00:27	1.1
	06:37	7.6
	12:47	1.5
	18:57	7.8
15 Oct 2018	01:15	1.4
	07:26	7.3
	13:37	1.8
	19:48	7.5
21 Oct 2018	00:35	7.5
	06:48	1.7
	12:59	7.4
	19:10	1.7
23 Oct 2018	02:00	7.8
	08:10	1.2
	14:19	7.9
	20:31	1.1
25 Oct 2018	03:17	8.1
	09:27	0.9
	15:35	8.3
	21:49	0.7
5 Nov 2018	00:47	8.3
	07:02	0.7
	13:14	8.4
	19:30	0.6
29 Nov 2018	01:39	0.8
	07:53	8.0
	14:08	1.2
	20:20	8.2

Table 1: Tides at Digby. <http://www.tides.gc.ca/>

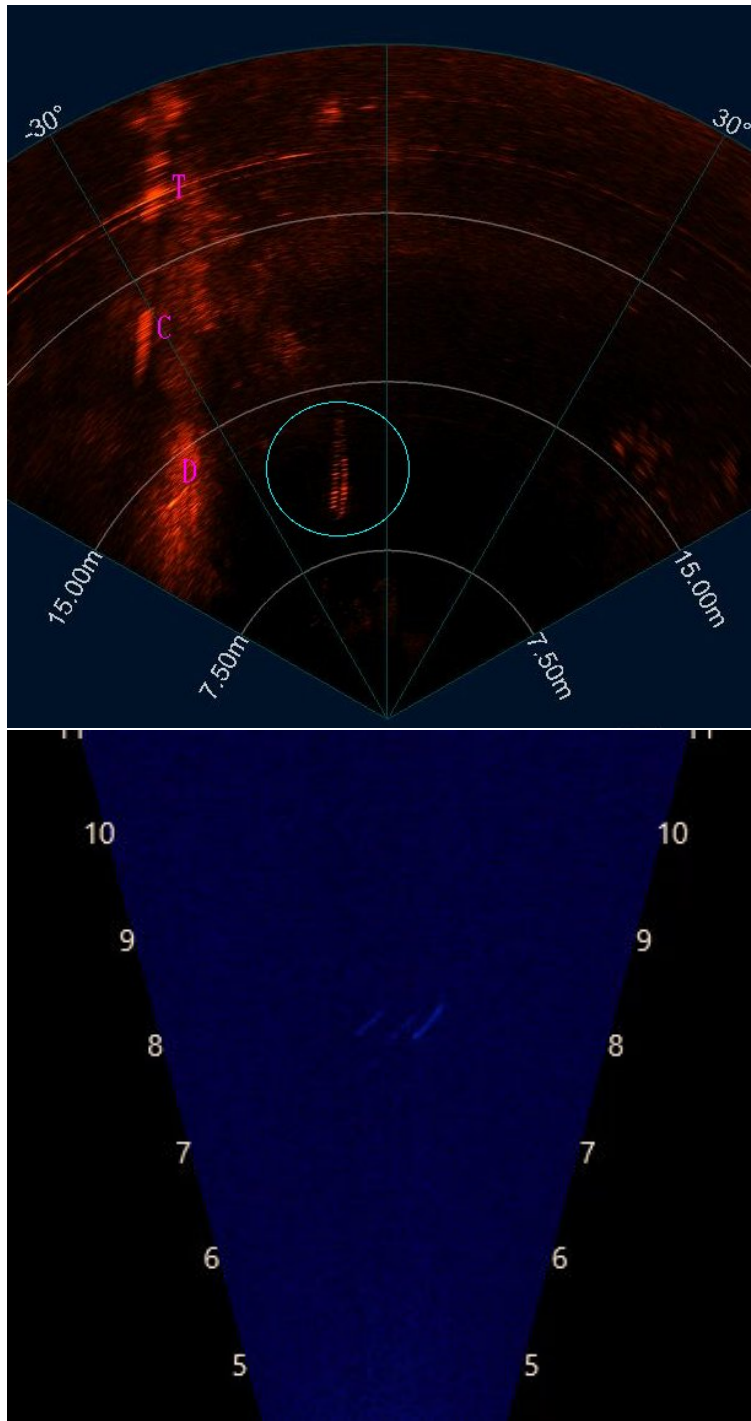


Figure 19: TOP: Image obtained (1707 UTC on 23 October 2018) by the Gemini 720is with a persistence filter to obtain the recent track of the target (circled). The herring and shackle appear as parallel line segments. BOTTOM: a snapshot of the same target, a short time later, as obtained by the Aris.



Figure 20: TOP-LEFT: Aris image of the target (shackle with line to a 20 cm herring) at 4.5 m range. TOP-RIGHT: GOPRO image ( $3840 \times 2160$  pixels) showing the target at 3.3 m range. BOTTOM-LEFT: Zooming in on the 20 cm herring, full resolution of the GOPRO. BOTTOM-RIGHT: Same image as to the left, except that the pixel size is increased by a factor of 2. Measurements were made at 1912 UTC on 23 October 2018.

view of both the Aris and the GOPRO camera. Also, by this time the tide was beginning to slow, approaching low tide. Again, Gemini tracked the target throughout its large field of view. Figure 20 shows images obtained by the Aris and GOPRO for the same cast of the target. The Aris image is not obtained at exactly the same time as the GOPRO image, but nearly the same time. At a range of about 4.5 m, the Aris obtains a clear image but not useful for species identification. Obviously, if the object is tracked for some time, then it might be possible to infer something from its motion [21, 22]. An Aris has a limited field of view so most targets will be swept by in short order. Hence, trajectory properties are more likely to be obtained from a sonar that has a bigger field of view (e.g., Gemini).

The GOPRO image in Figure 20 is obtained from a range of about 3.3 m (based upon the known length of the herring). The top right image clearly shows a fish attached by a line to the shackle. It is necessary to zoom in (lower left panel) in order to really see the fish. One can zoom in and see more detail because the resolution of the GOPRO is  $3840 \times 2160$  pixels which is more than can be resolved by a human eye looking at the image in the top right panel. The zoomed image indicates that clarity of water and droplets on the inside of the window of the camera case become factors limiting image quality.

At  $3840 \times 2160$  pixels, each camera image is memory intensive. Reducing the resolution by a factor of 2 (averaging over  $2 \times 2$  pixels) gives a somewhat pixelated image in the bottom right panel of Figure 20. The image still looks like a fish and it seems obvious that at greater range the inherent limitation would be visibility, not the number of pixels. It is also relevant to note that the higher resolution image (lower left) shows small features in the background surrounding the fish — perhaps relating to bubbles or material on the camera lens, or something on the window of the water tight case or small amounts of condensation inside the case. These small features blend into a uniform background with the averaging (and in lower resolution video, LRV, obtained directly from the camera). Previously, we have found it useful to use averaging operators when automating target detection.

### 3.2.2 Sonar/camera fish detection at PLAT-I

The Gemini 720is detected what appears to be a school of wild fish (Figure 21) at 1538 UTC on 23 October 2018, a little more than an hour after high tide (Table 1). This image was obtained during the first of the series of three target detect/tracking experiments reported above. Other observations of fish schools were made from time to time but we have made no effort to document them.

Given the deployment level of the Gemini (2.3 m below the sea surface) and a vertical beam angle of  $20^\circ$ , the school of fish must have been within 6 m of the surface. Measurements were made shortly after high tide, so the school was well clear of the bottom and at a level similar to that which would be swept by turbine rotors.

A diver inspected the PLAT-I mooring system at high tide (Table 1) on 25 October 2018. Video footage from the inspection is qualitatively instructive. Flounder, crabs and lobster are seen at the seafloor. Figure 21 shows an image of a school of fish swimming near the bottom, above the mooring chains.

Our measurement program was designed to measure targets during daylight hours and well clear of the seafloor. During daylight hours, it might be anticipated that fish are more commonly near the seafloor. Nevertheless, sometimes fish are observed near PLAT-I and at the depth of the turbine rotors.

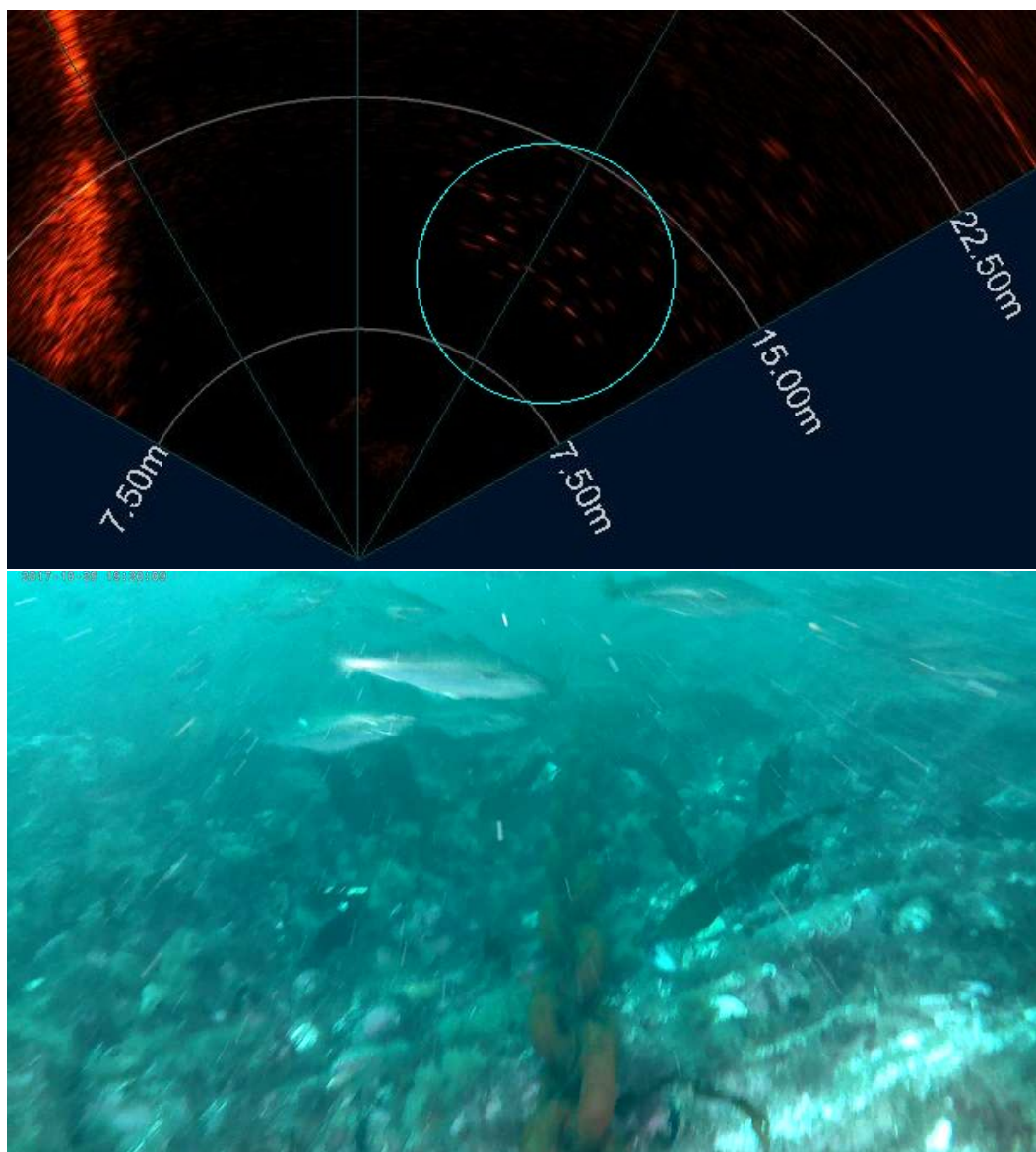


Figure 21: TOP: Gemini 720is image showing a school of fish on 23 October 2018, 1538 UTC. BOTTOM: Dive camera image showing a school of fish above the PLAT-I mooring chain 25 October 2018, 1920 UTC. Dive camera footage provided by SME.

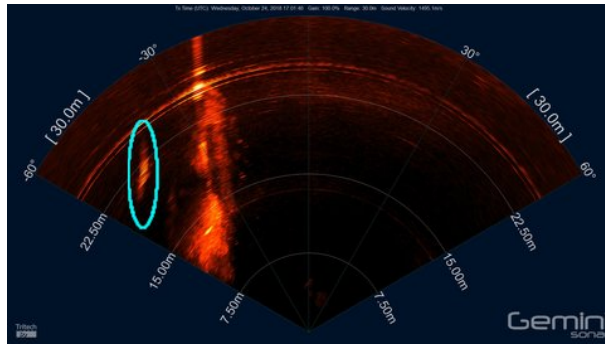


Figure 22: The cyan circle indicates the track taken by a shackle target, as seen using the Gemini 720is with a persistence filter.

### 3.2.3 Target tracking across the central hull, 24 October 2018

On 24 October 2018 we tested the ability of the Gemini 720is to detect the shackle target (suspended from the surface float) when it was cast off the port bow of the central hull with the Gemini mounted on the starboard hull, as before. Thus, the Gemini is viewing a target that is on the far side of all the interference caused by; the centre hull, mooring hawsers/chains, the heat diffuser, and the turret (Figure 13). Figure 22 shows a portion of the track taken by the shackle, as seen by applying a persistence filter. The target was seen for every cast, although the signal was not so clean as when the target and Gemini are both on the same side of the central hull.

Clearly, the central hull and mooring infrastructure cause a great deal of interference when they are within the beam of the sonar. This interference does not necessarily prevent a human observer from discerning targets within sonar images. We expect, however, that such interference should be avoided if there is any thought of automating detection of targets within sonar images.

### 3.2.4 Rotating the Gemini 720is, 24 October 2018

On 24 October the Gemini was rotated through 90° so its 512 beams spanned 120° in a vertical plane and the 20° spreading of each beam was in the horizontal. Casts were made with the surface float and shackle target system and also by tossing a rock into the ocean. The experiment and results are presented in a HTML document with hyperlinks to ecd, mp4, and wmv movie files [32]. Here the discussion will be limited to a few still images (Figure 23) obtained from the data set.

The top panel in Figure 23 is an image from the rotated Gemini that shows background signals (no target). A signal return from the surface is clear and shows the Gemini is about 2 m below the surface. Very near the Gemini,  $\leq 3$  m, there is a very strong surface reflection as well as a reflection from about 0.5 m below the surface. This reflection is associated with the starboard hull (which we mount to) and is sufficiently strong to cause visible side lobes that extend in the angular direction.

At about 25 m range, the turret returns a strong signal that shows side lobes spread through a wide range of angles (Figure 23). The forward mooring hawser/chain extends from the turret. A strong return from near the heat diffuser is evident near the letter ‘f’ of the label ‘Surface’. The structure causing that return has not been identified.

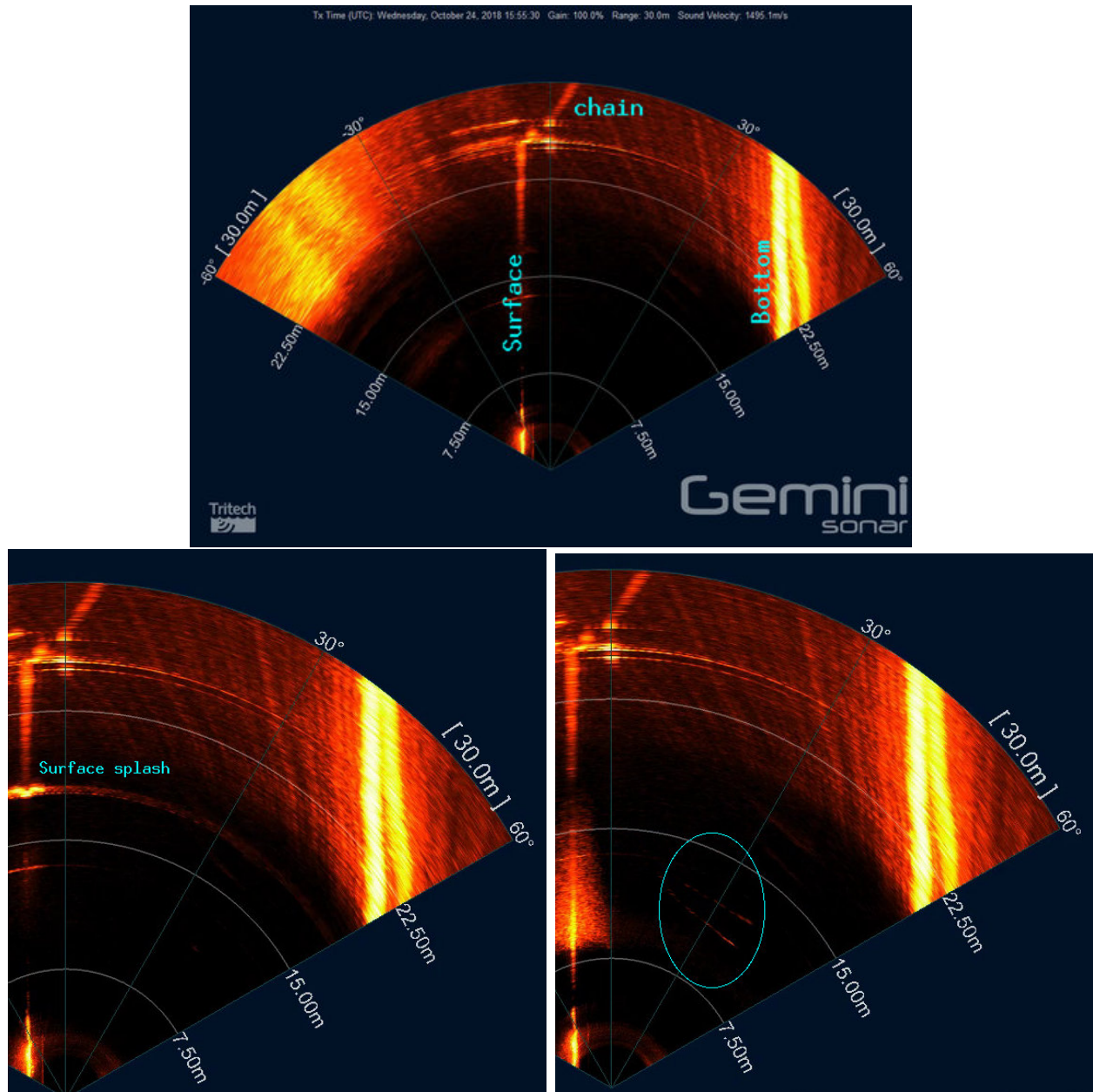


Figure 23: Images obtained with Gemini rotated 90° so that it measures range and angle in the vertical plane. TOP: Signals returned from sea surface, seafloor, and PLAT-I mooring system. LOWER LEFT: A strong surface splash is seen as a rock target enters the water and bubbles cause side lobes through the angular (vertical) dimension. LOWER RIGHT: A short time later, a persistence filter is used to visualize the track of the sinking target. Signal paths reflected from the sea surface cause a ghost target at slightly greater range.

The bottom appears as two very strong lines, extending from a range of about 20 m (Figure 23). The two lines are separated by a distance that corresponds to two paths from the Gemini to the bottom: (a) a direct path, and (b) a reflection from the sea surface. Note that the background signal is quite clean.

The lower left panel in Figure 23 shows the signal return when a rock splashes into the water. It is a strong return with side lobes evident through the angular dimension. Bubbles from the splash are evident near the surface as they propagate downstream (right panel) but do not contaminate the signal at depth. A persistence filter was used to see the rock and its recent track (inside the cyan ellipse in the right panel) as it falls through the water column and is swept downstream by the current. It appears that there are two targets. The closest target is the real thing, with a phantom target further away that is caused by the rock being illuminated by a signal reflected from the sea surface.

The second return signal (phantom target) might be avoided by orienting the rotated Gemini so that the top of its field of view does not intersect the air-water interface. Certainly, this would seem to be possible in deeper water. In the shallow waters of Grand Passage it merely replaces one problem with another: signals scattered from the bottom would confound target signals. On the other hand, the Aris only has a 30° spread in its beams. Thus, for Grand Passage, the Aris could be mounted with a 90° rotation and used to resolve the vertical coordinate of approaching targets.

### 3.2.5 A configuration for effective monitoring of fish-turbine interaction

The present project did not extend to environmental effects monitoring. Nevertheless, it was intended that the work would inform how effective environmental effects monitoring should be done. It is appropriate at this stage to consider effective environmental effects monitoring as it applies to fish interaction with in-stream turbines.

Better mounting systems are required in order to obtain high quality measurements.

- The mounts must be capable of getting instruments to depths approaching that of the turbines axis of rotation. Also, mounts are required to locate instruments at locations other than the inside edge of the outer hulls.
- The mounts have to be stable and vibration free.
- The mounts must allow instruments to be quickly deployed and recovered. Biofouling (or fouling by other material) is a serious problem for cameras so regular servicing is required.

Instruments might be mounted in a configuration similar to that shown in Figure 24. This improves on our test configuration (Figure 18) in several ways. First, mounting the Gemini 720is on the bridge gives coverage by the sonar beam that extends over much of the area swept by the rotor and from positions immediately in front of the rotor to far upstream (lower-right panel of Figure 24). In particular, the Gemini monitors the lower portion of the area swept by the rotor on the expectation that fish are less likely to be very near the air-water interface. The top of the beam cleanly passes well beneath the port hull. Monitoring on the port side avoids difficulties associated with the heat diffuser. The beam is also oriented to avoid reflections by the PLAT-I and its mooring system while well resolving trajectories that pass around the area swept by the turbine rotor. This configuration allows targets to be tracked from well

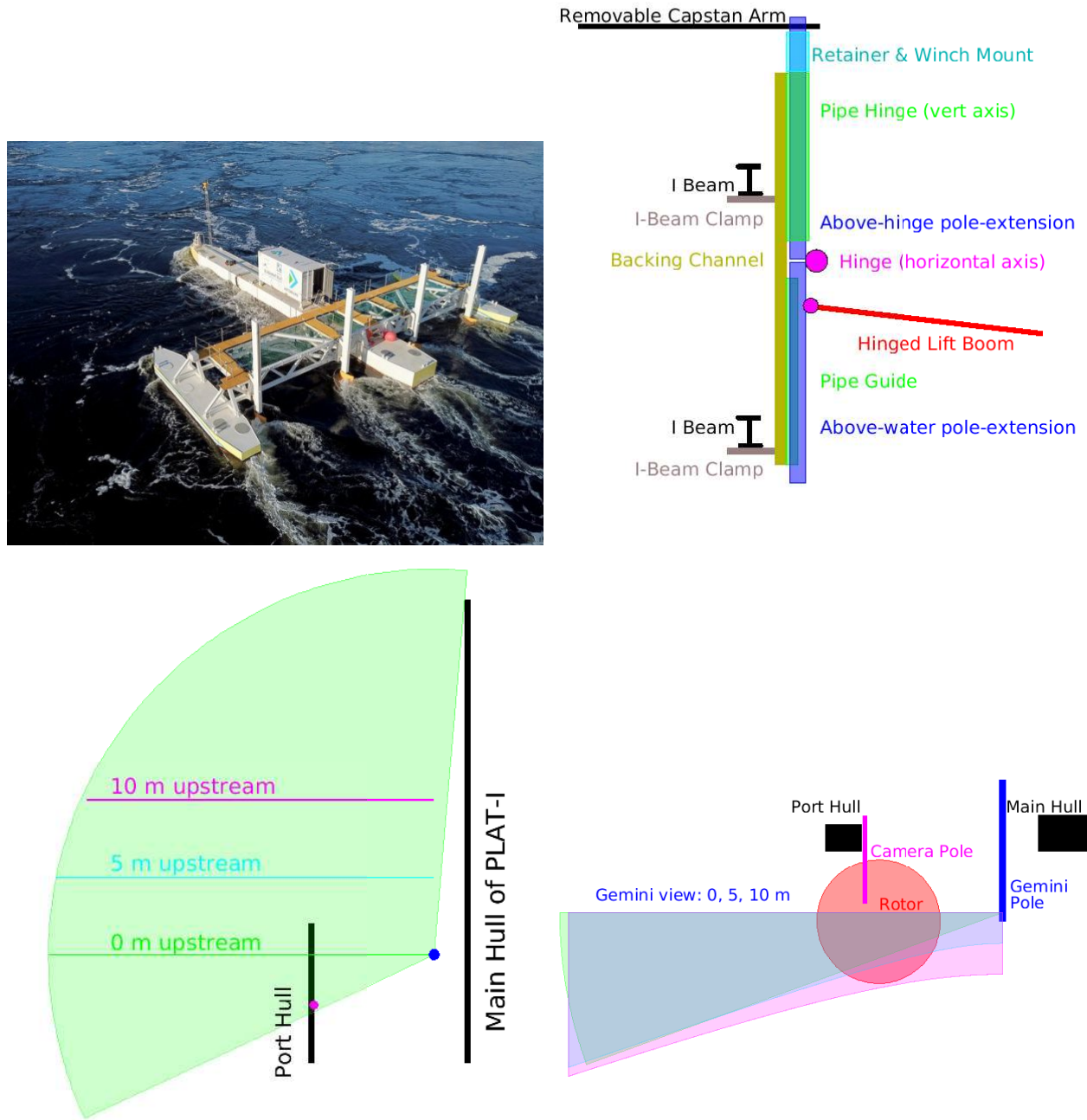


Figure 24: The best field of view is obtained by mounting the Gemini 720is sonar to the bridge. TOP LEFT: Photograph of PLAT-I. TOP RIGHT: Schematic for the above-water portion of a third-generation instrument mount that can be attached to the I-beams of the bridge. BOTTOM LEFT: Plan view of the Gemini beam when mounted from the bridge. BOTTOM RIGHT: View from astern of vertical sections through the Gemini beam. Different shadings are used to illustrate the beam coverage at distances 0, 5, and 10 m upstream.

upstream so as to observe avoidance behaviour. It gives the best possibility of obtaining low-noise images which will be a minimum requirement for semi-automated target detection.

Rotating the Aris would enable avoidance to be measured for targets that move vertically. The Aris has multiple beams spread over  $30^\circ$  so rotating it to resolve depth and range should be possible without causing spurious reflections from either the sea surface or the seafloor. The Aris could be mounted with the Gemini, looking towards port to measure the area in front of the rotor and beneath the port hull. The combination of Gemini and Aris would enable three-dimensional positions to be established for targets in that area. Essentially, that combination of instruments becomes an acoustic stereo-camera. This combination has utility at nighttime which would allow comparison of day-night detections.

Targets that do not avoid the turbine can be expected to pass through the field of view of an optical camera, and thus be identified. Assuming the turbine blade can be sufficiently resolved (it was not installed when our measurements were made), then two synchronized cameras could be mounted to look at the rotor area so as to have stereo vision. This can be achieved by mounting the cameras at different depths on one pole. Stereo vision is required in order to resolve trajectories of targets that go through the area swept by the rotor. Thus, it may be possible to say something as to whether or not the targets make contact with the blade, although such images are unlikely to determine whether or not such a target is damaged.

It is critical to understand the limitations of optical camera measurements. Certainly, we might confirm that *a marine animal has been harmed* if the video image shows some obvious mutilation. If an animal is visually unscathed as it passes through the turbine then this does not mean that it wasn't harmed by jarring, or shear forces, or pressure changes. To demonstrate no harm, we would have to capture the animal downstream and monitor it — without damaging it in the process of examining it. Presently there is no way to do such things. If no animals are seen passing through the area swept by the blade then that might just mean that animals were not around when the camera footage was obtained, or that methods for interpreting the video data [24] are inadequate.

As mentioned in the introduction, it is not adequate to analyze only a small subsample of video camera observations. Animal abundance is patchy and low. Cameras monitor a tiny area, so most of the time we should expect that fish will not be present in camera images. One of the great advantages of the Gemini sonar is that targets are detected over a large area and their persistence tracks will be apparent for a long period of time. The time frame for a target to pass the field of view of a camera is at least an order of magnitude shorter than that to pass through the field of view of the Gemini sonar. Even without automated detections, it would be an order of magnitude faster for a human to scan clean Gemini images than optical camera images.

Video and sonar pointing upstream are required for confirmation that animals were present and to demonstrate adequate detection methods. Indeed, we have found it relatively easy to automate target detection<sup>4</sup> when a camera is viewing open water. Thus automated target detection in an image from a camera looking upstream would be an effective method for directing a human effort to detect targets in a more complex image obtained from a camera that might have a turbine rotor in its field of view.

Far more important, video and sonar pointing upstream are indispensable for measuring the extent to which marine animals modify their trajectories to avoid the area swept by rotors.

---

<sup>4</sup>Perhaps we should say “semi-automated target detection” because a scientist must always carefully check what has been “found”.

Measuring avoidance is probably the only method that we presently have for placing some bounds upon the risk that a turbine mounted to PLAT-I will pose to marine animals in Grand Passage. Measurements far upstream detect those animals that might encounter the turbine and measurements nearer the turbine show what fraction of these animals avoid the turbine.

## 4 Interactions of active and passive acoustic devices

Cape Sharp Tidal's 2016-2017 deployment of an Open Hydro turbine at FORCE incorporated both active acoustic devices (500 kHz ADCP, 720 kHz sonar, ADV and acoustic modem) and passive acoustic hydrophones on the same platform. Emissions from active acoustic devices were strongly evident in the hydrophone record. The intent of *STREEM* was to quantify how imaging sonar affects the passive acoustic hydrophone measurements.

### 4.1 Drifting hydrophone array with sonar (on/off): interference

The 19 October 2018 target detection experiment (see §3.1) utilized two synchronized icListenHF hydrophones on the target-drifter. Our previous analysis considered those hydrophones as targets to be detected by the Gemini 720is imaging sonar. Here we consider how the icListenHF hydrophones detect transmissions from the Gemini 720is imaging sonar. Our analysis is slightly complicated by the fact that a HR Vemco fish tag was placed on the target-drifter, between the hydrophones.

The experiment used a Gemini 720is mounted to the stern on the port side of RV Puffin. The method was to drift away from the target float while using oars to orient the boat and keep the Gemini 720is pointed at the hydrophones. Six drifts were used to determine how Gemini 720is emissions (nominally transmitting at 720 kHz) were detected by the icListenHF broadband hydrophones (10 Hz to 256 kHz). The drifts were made with three different gain settings on the Gemini (100%, 50% and 10%) and for hydrophones at two depths (5 m and 10 m). The Welch method was used to obtain power spectral density (PSD) for hydrophone measurements during each one second interval as the boat drifted away. Distance from the boat to the target was similarly obtained for each second. For each drift, PSD were accumulated as a function of separation distance in 5 m bins.

Results did not depend upon gain setting of the Gemini 720is, as expected. Neither did they depend upon the depth of the hydrophones. Figure 25 shows power spectral density when the Gemini 720is is near the icListenHF's and when it is far from them. A narrow peak at 180 kHz has amplitude that is independent of separation of the Gemini from the hydrophones. This is caused by the Pulse Position Modulation (PPM) signals from the Vemco tag which was attached between the two hydrophones on the target-drifter. A broader peak at 170 kHz is also independent of separation distance from the Gemini to the hydrophones. This is caused by 170 kHz HR signals that are transmitted by the Vemco fish.

Aside from the effects of the Vemco tag, Figure 25 indicates that the Gemini does transmit sound energy at frequencies in the range 50-250 kHz. To see this more clearly, we isolate PSD corresponding to times when the Vemco tag was not transmitting. Further, the sensitivity of the icListenHF varies with frequency and so a correction is made for that. Figure 26 shows the averaged PSD which now contain the isolated effect of the Gemini 720is. We might reasonably assume that the effect of Gemini on the hydrophone is small when the Gemini is far from the

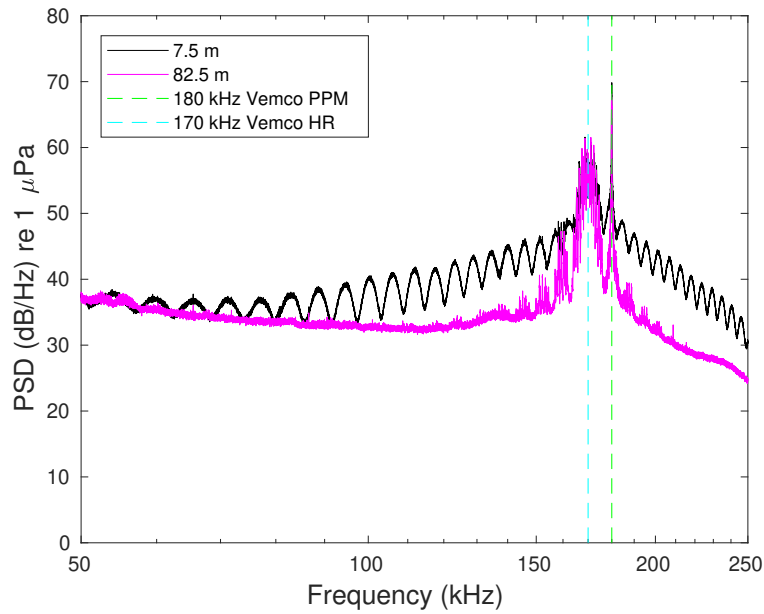


Figure 25: Hydrophone measurements with the Gemini 720is in St. Mary’s Bay. Two hydrophones and an acoustic Vemco fish tag were attached to the target drifter. The Gemini is mounted on a boat and pointed towards the drifter. Black line shows the power spectral density (PSD) for hydrophone measurements when the Gemini is at a typical range of 7.6 m. The magenta line shows the PSD when the Gemini is far away (typical range 82.5 m). No correction has been made for variation of receiver sensitivity with frequency.

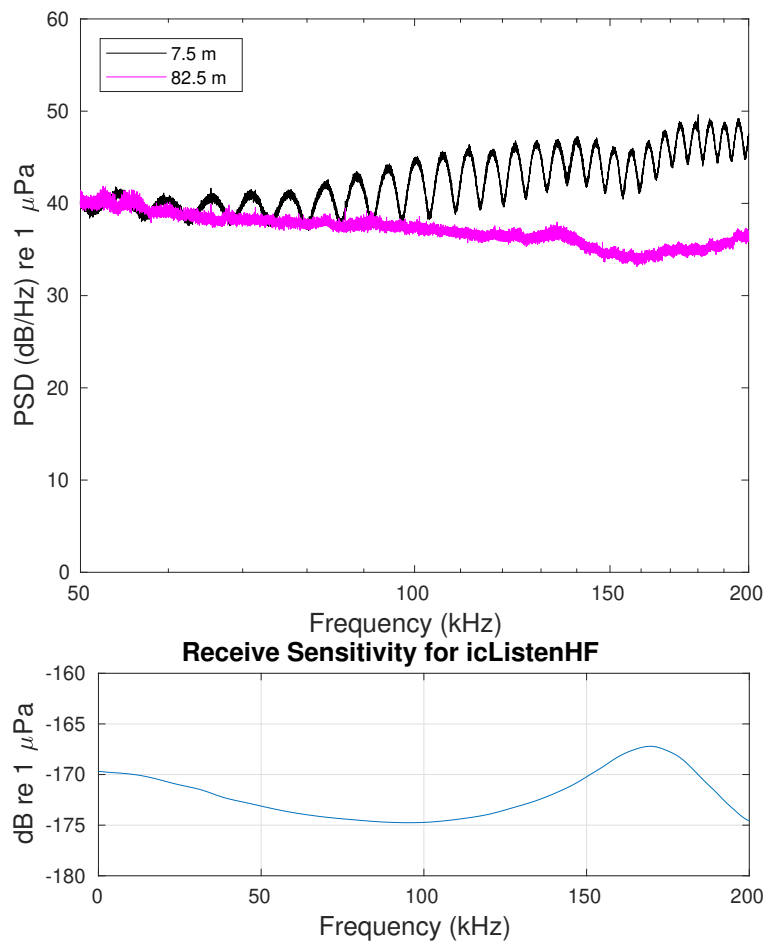


Figure 26: TOP: The black line shows PSD when the distance from Gemini to hydrophones was 5-10 m. The magenta line shows the PSD when the distance was 80-85 m. Here we have selected intervals when the Vemco fish tag is not transmitting. A correction has been made for receiver sensitivity. BOTTOM: Receiver sensitivity.

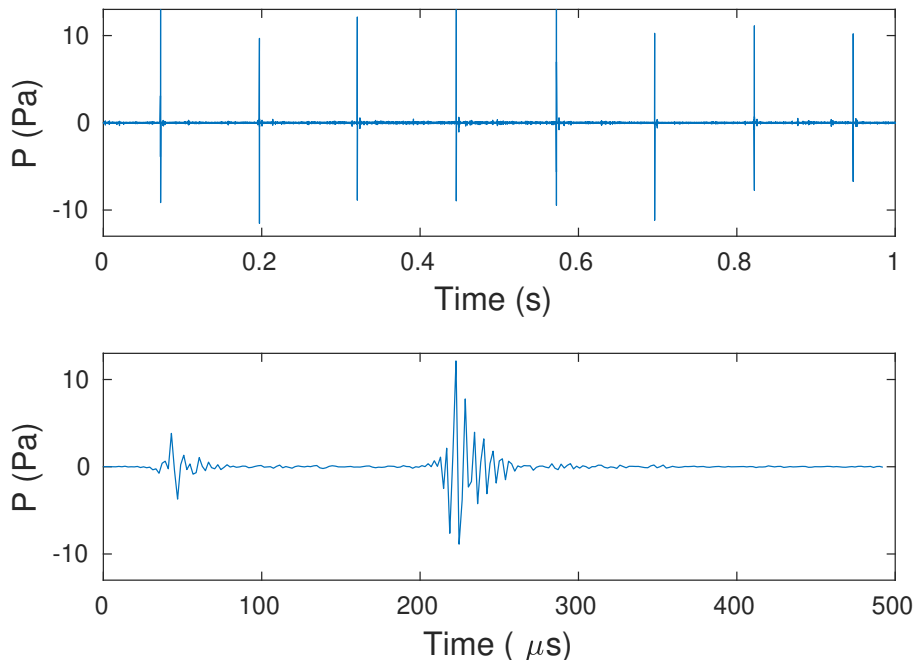


Figure 27: Hydrophone measurements with the Gemini in St. Mary’s Bay at a time when the Gemini was 7.5 to 12.5 m from the icListenHF hydrophones. Time series were high-pass filtered. Plots show the Gemini 720is signal as seen in the time domain by an icListenHF.

hydrophone. Thus, the magenta line in Figure 26 might be considered to represent ambient levels. Hydrophone measurements made when the Gemini is nearby show PSD rising in an oscillatory way for frequency increasing above 50 kHz (black line in Figure 26).

High-pass filtering icListenHF hydrophone measurements that were made when the Gemini was nearby the icListenHF hydrophones enables us to see time series of the Gemini 720is signal (top plot in Figure 27). The signal appears as short pulses with an inter-pulse interval of about 1/8 s. Zooming in (bottom plot in Figure 27) it seems that each pulse is made up of two parts. Again, these pulses are of such short duration that they cannot be registered by the matched-filter part of the Coda algorithm [15] as false porpoise click detections. Nevertheless, like the 500 kHz ADCP, a 720 kHz Gemini causes background sound near the porpoise frequency-band and that will cause a secondary part of the Coda algorithm to reject weak porpoise clicks.

That portion of the Gemini signal that is in the frequency range that harbour porpoise perceive (Figure 27) has an amplitude of about 10 Pa at a distance 7.5 to 12.5 m. Adjusting signal amplitude for radial spreading and converting to decibels, gives a source level in the range 157-162 dB (re  $\mu\text{Pa}$  at 1 m). This source level is at the low end of the range of source levels that have been measured for harbour porpoise [33, 34, 35]. Clearly, porpoise can be expected to detect emissions from a Gemini 720is<sup>5</sup> so there is a need to measure how such emissions might change the behaviour of harbour porpoise (and, perhaps, some other marine mammals that have commensurate audiograms).

In theory, the Gemini 720is has a beam that spreads through 120° in the horizontal plane.

---

<sup>5</sup>Porpoise will detect many other active acoustic devices as well as emissions from other technologies used in the marine environment.

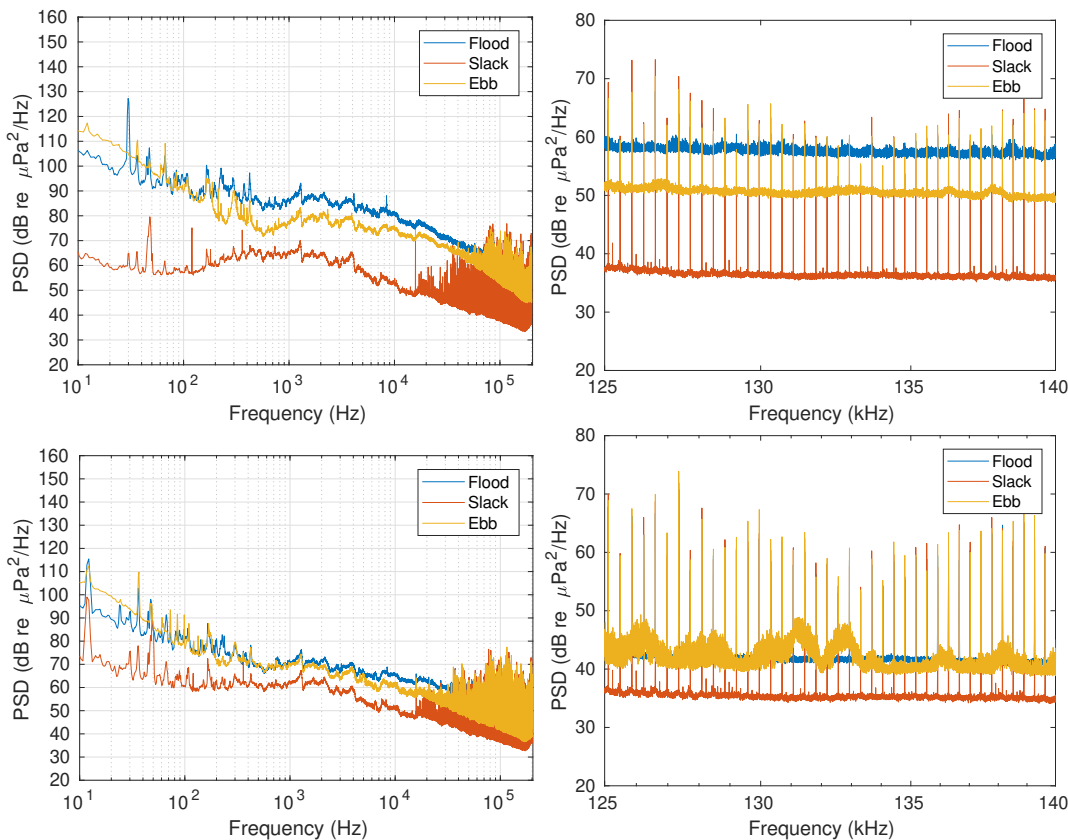


Figure 28: PSD obtained from icListenHF 1406 which was mounted to the western end of the OpenHydro platform at the FORCE Test Site in Minas Passage. During the 10 October 2018 spring tide (top) and the 18 October 2018 neap tide (bottom). We zoom in on the frequency band 125-145 kHz in the plots to the right.

Or, at least, that is the zone in which it makes measurements. Just as active acoustic devices have emissions at frequencies quite different from those that they use, we should be wary that they might have emissions in directions quite different from those that they measure! It would be good to test the extent to which hydrophones are effected when they are out of the nominal beam of the Gemini 720is. Our effort to make this measurement failed because strong winds prevented the boat from being controlled with the precision required.

#### 4.1.1 Comparison with hydrophones on the OpenHydro platform

The Integrated System for Environmental Monitoring (ISEM) project operated many active acoustic devices on the OpenHydro turbine/platform that was deployed at the FORCE Test Site in Minas Passage. It was not possible during the ISEM project to properly isolate the signals from each active device as they appeared in the icListenHF hydrophone records [18]. Making matters more complicated, ISEM found evidence that the turbine may also have been causing very high frequency sound when it operated [18]. One of the devices installed on the OpenHydro platform was a Gemini 720i. It is therefore useful to make comparisons with the STREEM measurements (see also, §5.4.1).

Figure 28 shows PSD from measurements made by an icListenHF hydrophone that was

fastened to the western end of the OpenHydro gravity-base platform at the FORCE Test Site in Minas Passage. Regularly-spaced, narrow-band spikes are a feature of these PSD and the spikes become increasingly apparent as frequency increases beyond 10 kHz. The cause of these spikes is a mystery. Such spikes were not present in PSD [13] obtained from measurements by icListenHF hydrophones that were attached to a Lander platform deployed on the seafloor at the FORCE Test Site for two weeks in June 2014 before turbines were deployed [36]. The spikes are most evident at slack tide (Figure 28), when ambient sound level is lowest at the FORCE Test Site.

The power spectral density (PSD) in Figure 26 does not exhibit large-amplitude spikes like those seen in Figure 28 for measurements made on the OpenHydro turbine/platform in Minas Passage. Based on Figure 26, it would seem that the Gemini has a more broadband signature that may be more difficult to discern from ambient sounds at the energetic FORCE Test Site. By process of elimination, it seems most likely<sup>6</sup> that the Acoustic Doppler Current Profilers (ADCPs) contaminated PSD with large amplitude, high-frequency spikes during the OpenHydro turbine/platform deployment. Although the ADCPs use frequencies near 500 kHz to measure currents, they obviously have sound emissions over a much wider range of frequencies, including frequencies that harbour porpoises use.

#### 4.1.2 Vemco tag: 180 kHz PPM signal

Figure 25 shows a broad peak in the PSD at 180 kHz which corresponds to the PPM signal transmitted by the Vemco fish tag that was attached between the two hydrophones during the 19 October 2018 target detection experiment (see §3.1). The PPM signal was transmitted at random intervals of 25-35 seconds. Each PPM signal being a set of eight 4 ms pulses that are separated by about 1/4 of a second. Hydrophone measurements of the PPM timeseries are shown in Figure 29. The top time series shows a sequence of eight pulse-modulated 180 kHz signals and the lower plot shows one of the pulses in more detail. The separation between arrival times of sequential pulses is used to encode information about the tag. Thus, this form of encoding is called pulse position modulation (PPM).

Each pulse is is a uniform amplitude signal containing many 180 kHz uniform amplitude oscillations over the 4 ms duration of the pulse. Thus the Fourier series representation of the pulse is dominated by a single mode at 180 kHz. The PPM signal is, therefore, seen as a sharp spike at 180 kHz in Figure 25.

Obviously, an icListenHF can be used to detect acoustic fish tags and the pulse arrival times can be obtained from such measurements [37]. Broadband hydrophones are commonly used for tidal power EEM in order to measure sound and detect marine mammal vocalizations. Specialized receivers are commonly used for tidal power EEM in order to detect acoustically tagged fish. Clearly, it would make EEM more effective if convenient procedures were developed for processing broadband hydrophone measurements to obtain detections of acoustically tagged fish.

#### 4.1.3 Vemco tag: 170 kHz HR signal

Figure 25 shows a broad peak in the PSD at 170 kHz. This corresponds to the HR signal that was being transmitted by the Vemco fish tag attached between the two hydrophones during

---

<sup>6</sup>But it is impossible to be sure of this because controlled tests were not done.

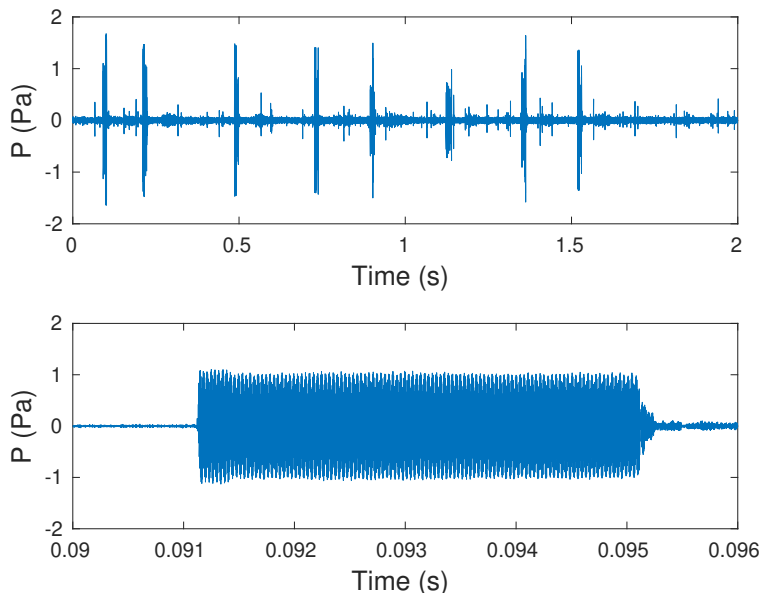


Figure 29: Hydrophone measurements with the Gemini in St. Mary’s Bay at a time when the Gemini was about 100 m from the icListenHF hydrophones. Time series were high-pass filtered. Plots show the Vemco 180 kHz PPM signal from a fish tag. PPM coding is based upon the interval between pulses.

the 19 October 2018 target detection experiment (see §3.1). HR signals are transmitted by the Vemco fish tag every 4-5 seconds. A time series of the 170 kHz HR signal is shown in the top panel of Figure 30. The duration of the HR pulse is about 6 ms. The amplitude of the pulse appears ragged. Zooming in on a portion of the pulse, we see abrupt phase changes. The HR signal conveys information using abrupt phase changes. In the frequency domain, this additional information appears as Fourier modes about the 170 kHz carrier wave. HR fish tag signals will therefore appear as a broader peak in the PSD than do the PPM signals (Figure 25).

It would probably be difficult to undertake signal processing of broadband hydrophone measurements to obtain information conveyed by HR signals. On the other hand, one of the reasons for using HR tags is so that an array of HR receivers can be used to obtain the position of a tagged animal near an in-stream turbine. For this purpose, a broadband hydrophone can be readily used to obtain additional signal arrival times. Again, there is a clear synergy between the two methods required for EEM. Effective EEM requires that the synergy be exploited.

#### 4.1.4 Detection of a Transmitting Vemco Tag by Gemini 720is

Previously, in Figure 9, we saw that the Gemini 720is accurately detected the position of a Vemco HR tag when it was not transmitting. The 19 October 2018 target-drifter experiment included 7 drifts that had Vemco 180/170 kHz tags attached on the target line. Gemini had gain set to 100% for drifts 1 and 5 and images obtained during both drifts sometimes had randomly located rectangular detections (like that at 25-30 m in Figure 31). The signal was not seen on the other drifts, when gain was either 50% or 10%, although that might just be

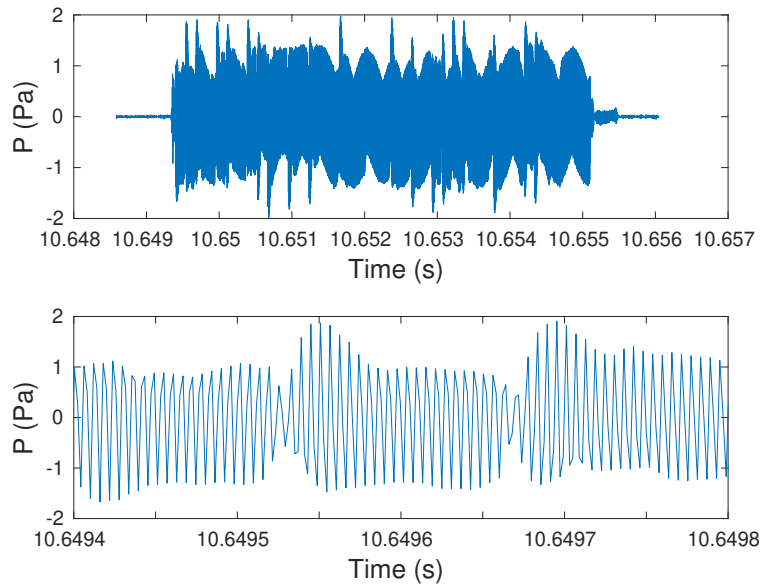


Figure 30: Hydrophone measurements with the Gemini in St. Mary’s Bay at a time when the Gemini was about 100 m from the icListenHF hydrophones. Time series were high-pass filtered. Plots show the Vemco 170 kHz HR signal from a fish tag. HR coding uses abrupt phase shifts within a single pulse.

a matter of coincidence rather than physics. GPS time synchronization of the hydrophones was not available at the time of this experiment. Nevertheless, examination of the icListenHF records indicated 180 kHz PPM signals within a second of these “rectangular detections”. Given that 720 kHz is a harmonic of 180 kHz, it seems quite likely that the Gemini 720is is detecting the 180 kHz PPM signal transmitted by the Vemco fish tag.

The 180 kHz PPM signal has pulses with duration 4 ms. Given the speed of sound, this corresponds to a travel distance of about 6 m which might relate to the radial elongation of the detection in the Gemini sonar image (Figure 31). Most of the PPM pulses are not displayed as a target detected by the Gemini 720is. To be registered as a target, a signal must arrive with a time that corresponds to the expected lag since the Gemini transmitted. Such arrivals of tag transmissions are purely accidental because the timing of the tag is unrelated to that of the Gemini. Thus, the Gemini represents the position of a transmitting tag in a purely random way, mostly “off the screen”. Detection of a transmitting tag has a clearly identifiable shape which discriminates it from other targets that we have observed.

#### 4.1.5 Performance of a Vemco HR2 Receiver with an operating Gemini 720is

On 19 October 2018 we operated both a Gemini 720is and a Vemco HR2 receiver off the stern of RV Puffin. The Gemini was detecting targets on the target-drifter. The HR2 receiver was detecting a Vemco tag attached to the target-drifter. On drifts 1-3 the tag was 5 m below sea surface and on drifts 5-7 at 10 m. Positions of boat and target-drifter were both measured by GPS so we could determine time spent within 10 m distance increments from the HR2 receiver to the tag. Separation distance spanned ranges from 2 m to 100 m. Ranges 10 m to 90 m were most common and the separation of receiver from tag was always less than 100 m. The tag

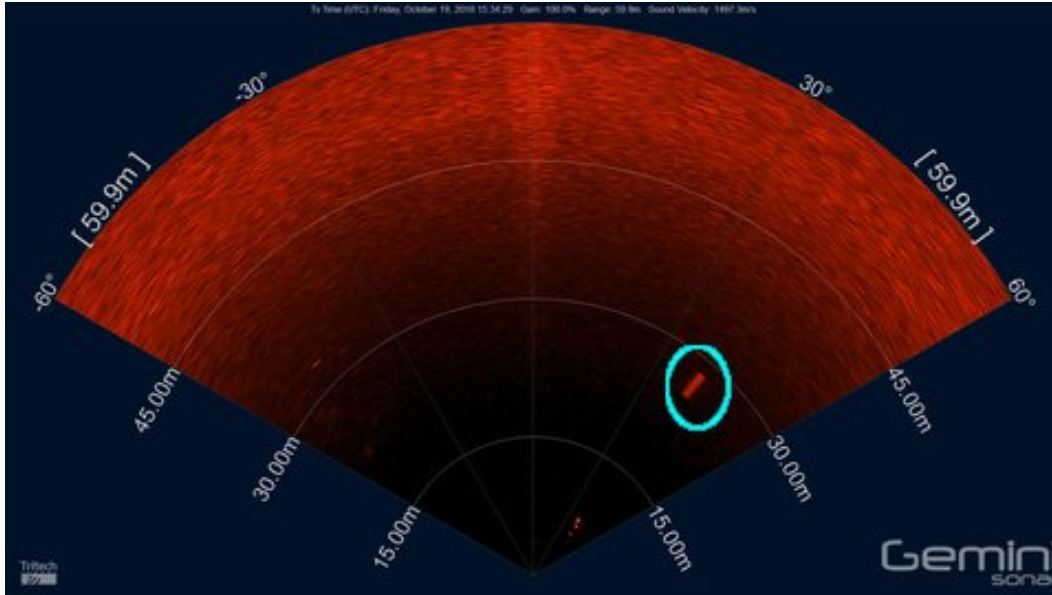


Figure 31: A transmission from a Vemco 180/170 kHz acoustic fish tag seems to be detected as a randomly placed block-like target (cyan circle). This image was from drift 1 on 19 Oct 2018 at 1534:29 UTC when gain was set to 100%. Note, such detections were not observed when gain was 50% and 10%.

Ranges (m)	HR Detection (fraction)	PPM Detection (fraction)
0-100	0.87	0.91
0-50	0.88	0.95
50-70	0.89	0.92
70-100	0.81	0.81

Table 2: Detection efficiency of a Vemco HR2 receiver when operating  $\approx 2$  m to the side of a transmitting Gemini 720is. HR are 170 kHz High Resolution signals that use phase shift encoding whereas PPM are 180 kHz Pulse Position Modulation signals.

transmitted a 180 kHz PPM signal at random intervals in the range 20-40 s, 30 s on average. HR signals were transmitted at intervals 4-6 s, 5 s on average. Given an elapsed measurement time it is therefore possible to obtain the expected number of transmissions. Comparing the number of transmissions received with the expected number transmitted gives an estimate of the detection efficiency.

Detection efficiency was generally high for both PPM and HR signals at the ranges measured (Table 2). Slightly better detection was achieved at ranges less than 70 m than at ranges greater than 70 m. These detection rates indicate that the HR2 receiver was not adversely impacted by operating a Gemini 720is nearby.

This gives some assurance that both HR2 receivers and an imaging sonar might be used to monitor fish from the same turbine platform at the same time. It should be stressed, however, that the HR2 receiver was not within the beam of the Gemini 720is.

Port Casts, 350 s			
Signal Type	# Expected	# Received	Fraction
PPM	11.67	10	0.86
HR	70	56	0.80
Starboard Casts, 375 s			
Signal Type	# Expected	# Received	Fraction
PPM	12.5	9	0.72
HR	75	51	0.68

Table 3: Reception of HR and PPM signals by an HR2 receiver mounted to the starboard side of the port hull of PLAT-I, Grand Passage.

## 4.2 Vessel-mounted hydrophone(s)

### 4.2.1 Performance of Vemco HR2 Receiver on PLAT-I

Results in §4.1.5 suggest that Vemco HR2 receivers might also be operated from an in-stream turbine installation (like PLAT-I) in order to detect and track any acoustically-tagged fish that pass by. To test detection of acoustic tags, the second-generation mount (Figure 15, bottom left) was used to attach a Vemco HR2 receiver (Figure 15, bottom right) to the port hull of PLAT-I. The HR2 receiver was deployed at a depth of about 3.5 m with the receiver oriented into the current in order to minimize non-acoustic noise [38], minimize drag, and not cause mount-pole instability. The HR2 receiver was set in place by 1632 UTC on 5 November 2018.

Acoustic transmitters were cast from the bow of PLAT-I in the same fashion as the fish target (Figure 17). A Maximum box served as a surface float with a shackle weight suspended 5 m below and the acoustic tag on a short leader from the shackle. The Maximum box was then attached to a casting line. The Maximum box, shackle and tag were cast from a position near the bow of the central hull and the tag was at a depth of about 5 m as it drifted downstream with the current. The tag was pulled back to the bow, and onboard, before it could reach the bridge that joins the hulls of PLAT-I. This was necessary in order to avoid entanglement with gear, particularly an ADV, mounted to PLAT-I.

Measurements were made near peak flood currents on a spring tide (Table 1). Casts towards the port side were made first, beginning around 1654 UTC on 5 November 2018. Then casts to the starboard side were made. An electronic stopwatch application on a smart phone was used to measure the total time that the tag spent in the water on each side (5 minutes 50 seconds to the port, 6 minutes 15 seconds to starboard). The tag was factory-configured to emit a PPM signal every 20-40 seconds, 30 seconds on average. An HR signal was transmitted every 4-6 seconds, 5 seconds on average. Thus, we could calculate the number of signals that we expected to be transmitted, and compare with the number received.

It is important to note that the tag was probably not subject to adverse conditions when it was drifting with the current. But the tag was dragged near the surface and often through disrupted water near the PLAT-I main-hull when it was hauled back onboard at the bow of PLAT-I. Thus, our measurements can be expected to under-represent the detection efficiency of tagged fish as they pass by PLAT-I.

The PPM and HR signals were detected with similar efficiency (Table 1). About 80% of HR tag transmissions were detected when the receiver and tag were on the same side of the

central hull, dropping to about 70% when tag and receiver were on opposite sides. Given the port location of the receiver, it was not surprising that the tag was better detected when it was on the port side of the central hull. On the other hand, the tag was quite well detected regardless of side and one might expect that the asymmetry would be even less for a tagged fish which would be expected to swim at a greater depth, away from the hull and bubble areas.

With slight modifications to the second-generation mounting system, one might anticipate that an array of HR2 receivers could be reliably mounted to PLAT-I. It seems likely that any tagged fish passing close to PLAT-I would be well detected by the array and its position could be determined. The array must be designed with care. Our experience with HR2 receivers elsewhere suggests that performance would be greatly degraded if the receiver is not mounted well clear of the reflecting surfaces of the PLAT-I hulls. That is one of the many reasons that the mounting system must be designed to support instruments at sufficient depth.

#### 4.2.2 The effect of echosounders on the Gemini 720is

On 13 October 2018 the Gemini 720is was mounted to the stern of RV Puffin at about 3.75 m below the sea surface. For a brief period the RV Puffin echosounding equipment was turned on. The effect on the Gemini imaging sonar was an intense return that spanned the azimuth and propagated radially at a swift rate. Figure 32 shows three successive frames obtained by displaying the Gemini data.

RV Puffin echosounding equipment consists of Raymarine Downvision and Fishfinder. Fishfinder uses frequencies 170-230 kHz and Downvision 320-380 kHz. Both these frequency ranges are well below the 720 kHz used by the Gemini 720is. Nevertheless, we should expect interference because it is becoming increasingly apparent that many active acoustic devices do not transmit a clean signal. In particular, we note that first harmonics of the frequencies used by the Downvision will include 720 kHz signals which Gemini is tuned to receive.

We have not measured the effects of other types of echosounding equipment on Gemini but it would be prudent, from an operational point of view, to begin with the assumption that they should be turned off whenever imaging sonar is being used to monitor marine animals. Indeed, the starting point should be that every active acoustic device will adversely effect other acoustic devices and/or affect marine animals [29, 39, 40, 41] — until demonstrated otherwise.<sup>7</sup>

#### 4.2.3 Echosounders and hydrophones

On 14 Oct 2018 we undertook icListenHF hydrophone measurements of signals from the Raymarine Downvision and Fishfinder that are installed on RV Puffin. Two synchronized hydrophones, separated by 2 m, were suspended from a vertical line attached at the stern of RV Puffin in such a way that the top hydrophone was at depths 1, 2, and 3 m below the surface. RV Puffin drifted while measurements were made. It turned out that acoustic signals from the RV Puffin saturated the hydrophone when it was at 1 or 2 m depth. The power spectral density plot (Figure 33) shows a huge signal that we associate with the 170-230 kHz band

---

<sup>7</sup>As previously mentioned, our tests indicated no obvious interference between the Gemini and Aris imaging sonars.

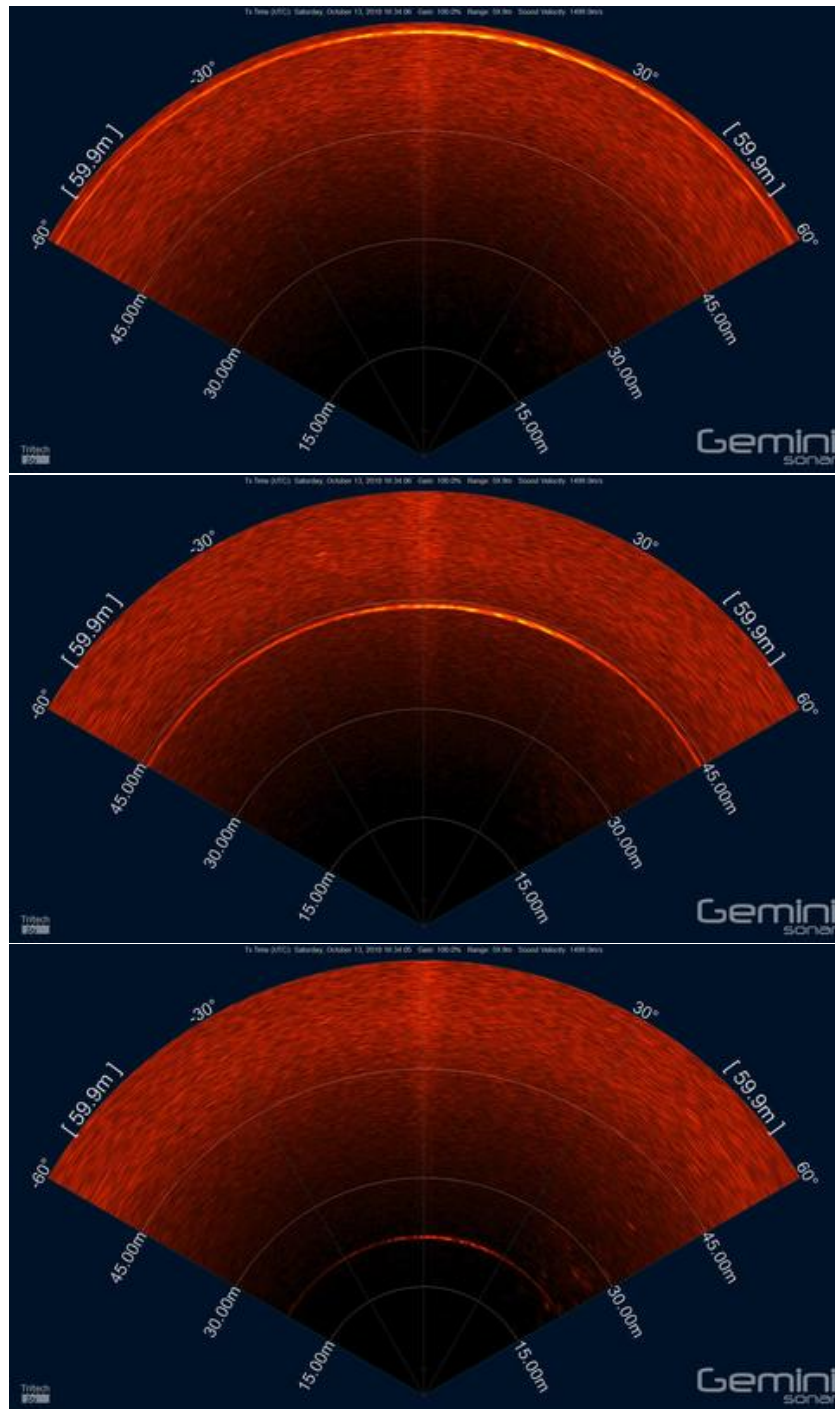


Figure 32: Effect of RV Puffin’s Raymarine Downvision and Fishfinder on Gemini 720i sonar image. Successive frames are shown bottom to top (13 October experiment). The echosounder/fishfinder causes signal that is spread over the angular dimension and propagates outwards along the radial dimension.

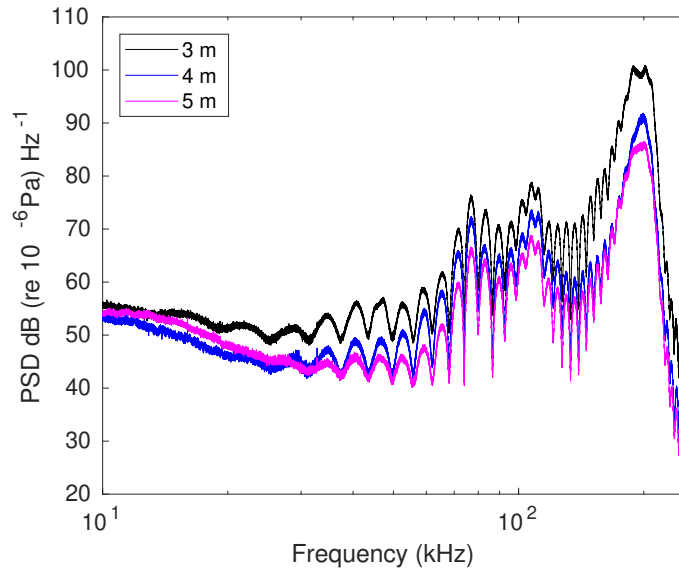


Figure 33: Hydrophone measurements of the Raymarine Downvision and Fishfinder used by the RV Puffin. PSD are plotted for hydrophones at depths 3 m (black), 4 m (blue) and 5 m (magenta).

used by the Fishfinder. In addition, the Raymarine system caused a good deal of acoustic energy at lower frequencies to which many marine mammals might be sensitive.

Timeseries (Figure 34) show that pulses from the echosounding equipment have characteristics quite different from typical clicks by toothed marine mammals (e.g., harbour porpoise) so they are expected to be separable in this regard from the signals which we intend to detect. On the other hand, acoustic transmissions from the RV Puffin’s Raymarine Downvision and Fishfinder are so powerful that they might still be expected to be disruptive to any measurement program. Indeed, active acoustic devices may be disruptive to some marine mammals [29, 39, 40].

When monitoring or scientific measurements are in progress, it is preferable that nearby service vessels operate without echosounders and fish finders.

#### 4.2.4 Sound projector and other anthropogenic sources

An icListenHF hydrophone was suspended from PLAT-I at high tide (Table 1) on 14 Oct 2018. Measurements for 1 minute, beginning at 1901 UTC, illustrate much anthropogenic contamination of the acoustic environment. RV Puffin had Downvision and Fishfinder operating, and these loom large at higher frequencies in the spectrogram (Figure 35). JASCO and Dalhousie University operated various moored sound projectors that appear as monotones and sweeps at frequencies in the range 7-18 kHz (Figure 35).

Anthropogenic noise at lower frequencies is not obvious from perusal of the spectrogram (Figure 35) but can be discerned by listening to the recording. Recognizable audible sounds included:

- Sound of the generator running on PLAT-I.
- The engine of the RV Puffin which had been left running.

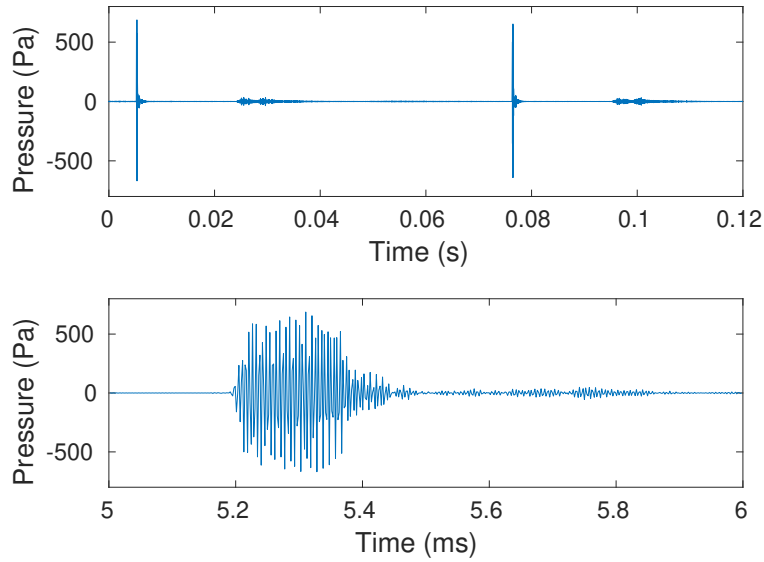


Figure 34: An illustrative example of the high-pass time series that shows acoustic transmission from the Raymarine Downvision and Fishfinder on RV Puffin.

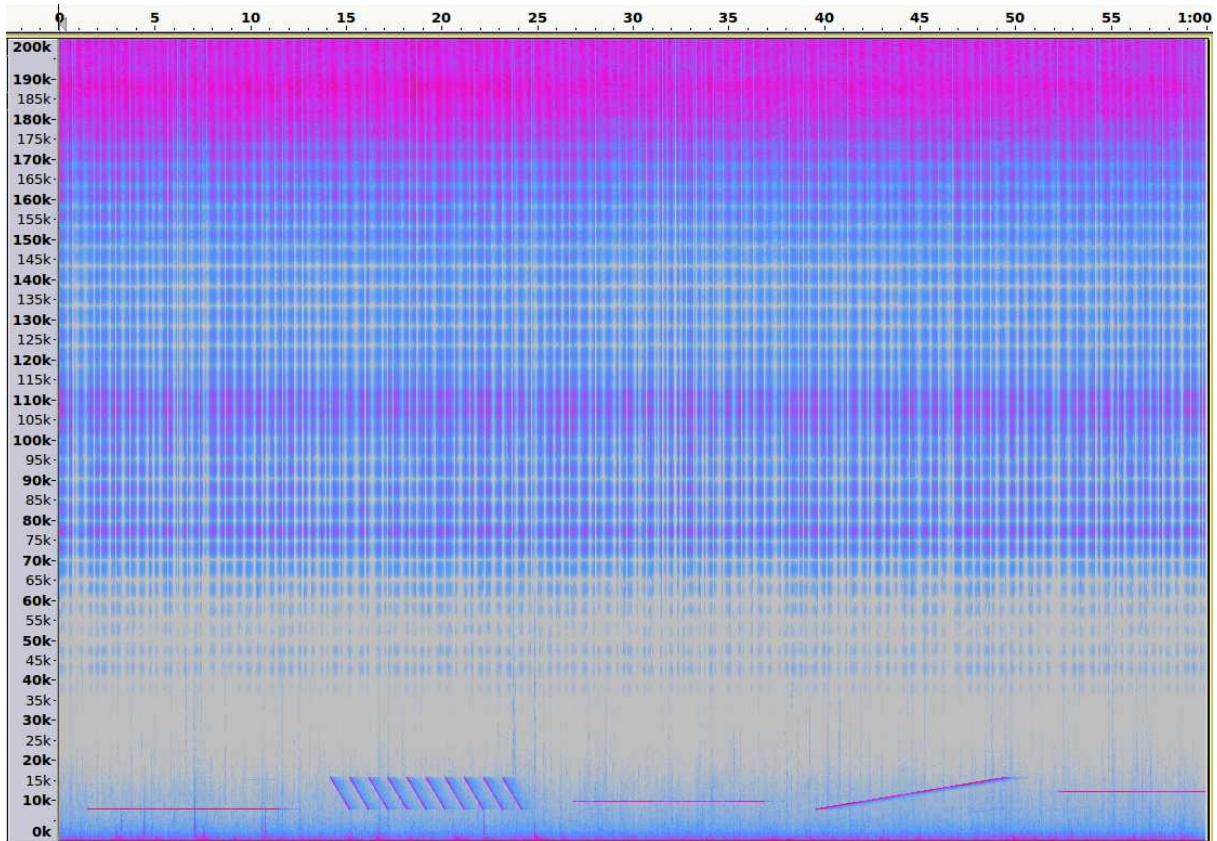


Figure 35: Spectrogram of measurements made at 1901 UTC (14 Oct 2018) using a hydrophone suspended from PLAT-I.

- Banging noises associated with flexing of the hull or perhaps movement of the turret and mooring components as PLAT-I turned with the tide.
- Water trickling/sloshing associated with current-hull and wave-hull interactions.

#### 4.2.5 Concurrent Operation of Gemini 720is and Aris

A qualitative experiment was undertaken on 23 October 2018 to determine whether the Aris sonar had any obvious effect on the Gemini 720is sonar. The Gemini was mounted to the starboard hull of PLAT-I, at a depth 2.3 m, and oriented so the beam was pointing forward (towards the bow). The Aris was mounted about 1.5 m to the stern of the Gemini, at slightly less than 1 m depth, and also with its beam directed forwards. A variety of qualitative experiments were undertaken using the two instruments with various settings. It did not appear that the Aris had any deleterious effect on the operation of the Gemini 720is.

Later in the day, both Gemini and Aris were used to identify targets cast off the PLAT-I §3.2. Both imaging sonars detected targets well and there was no obvious interference of one with the other. **We conclude that it is advantageous to use these instruments together, given that Gemini has a large range and wide field of view whereas the Aris obtains high resolution images when targets are close and within a more narrow field of view. Also, the fact that the Aris has a narrow field of view means that it can be operated with a 90° rotation in order to measure range and the vertical dimension.**

## 5 Soundscape, the turbine platform and porpoises

Sounds and other pressure vibrations that are made by an operating turbine might influence the behaviour of marine animals. It is, therefore, necessary to measure these sounds and vibrations in order to support any observations of animal behaviour that might be deduced from sonar and optical camera measurements.

### 5.1 Hydrophone measurements using the pad-float

A surface drifter that suspends sub-surface hydrophones can obtain measurements along a trajectory that passes nearby a turbine. This method is relatively easy to use for gravity-base, sub-surface turbine installations, as hydrophones can be drifted close over the top of the turbine [20]. The advantage of this method is that it enables a spatial gradient to be established as range to a sound source at a known location varies. In the case of an operating turbine, the location of the sound source might be fairly assumed. But to confirm the location of a sound source, one would need the drifter to carry an array of hydrophones and to also be fitted with GPS positioning and a compass for orientation.

Building a drifter that can safely carry an array of hydrophones through and around the PLAT-I, and obtain high-quality measurements, is something of a challenge. Figure 36 shows the prototype, which we shall call the “pad-float hydrophone array”. The broad circular float is designed to rotate around any obstacles and protect hydrophones from impact. A GPS/compass is attached to the top of the pad-float, so orientation and position are obtained.



Figure 36: LEFT: Pad-float hydrophone-array on a wooden stand, showing Smart Cable and GPS/compass above and hydrophones below. RIGHT: Deployed and passing between the hulls of PLAT-I. Photo credit: Mike Adams.

ABS plumbing extends through the pad-float so the hydrophone array is fixed below and connected with a Smart Cable above.

The pad-float is designed to carry a hydrophone array directly over turbine rotors which sweep within 1.5 m of the surface. Having hydrophones so near the surface results in measurements being made very near to any spilling surface waves, which can be locally noisy. Thus, the pad-float hydrophone array should only be operated in calm conditions. Of course, calm conditions are also best for isolating the turbine sounds from other sound sources.

Pad-float hydrophone measurements were made on 21 October 2018. The method was to use a boat to deploy the pad-float well upstream of the PLAT-I, then quickly navigate the boat across the current and turn off the engine. In this fashion, the boat would drift quietly clear of the PLAT-I and the pad-float would drift through the PLAT-I location. The right panel of Figure 36 shows a photograph taken from the bridge of PLAT-I as the pad-float passes underneath.

Currents in Grand Passage are variable, with large swirling eddies. In addition, PLAT-I has a tendency to swing about relative to the current direction which makes it difficult to determine an upstream deployment position that will see the pad-float pass close by a particular part of PLAT-I. Figure 37 shows 31 drifter tracks that are referenced relative to the position of PLAT-I. (The position of PLAT-I was measured with a Garmin GPS and its average value for each drift track is taken as the origin of the coordinate system.) While a few of the drifter tracks clearly missed their mark, this would not be a problem for our ultimate application because we also need some control measurements further from operating turbines. Most drifter tracks passed close by and between the hulls of PLAT-I.

At least one drifter track hit the bow of PLAT-I's central hull. No ill effect came of this, other than the sound of plywood bumping many tons of steel. The pad-float, being circular, stayed perfectly upright as it rolled around the bow of the central hull. On two occasions, the pad-float ran into the bow of the port hull. Again, to no ill effect.

There was a long swell running into Grand Passage on the test day and this was identified

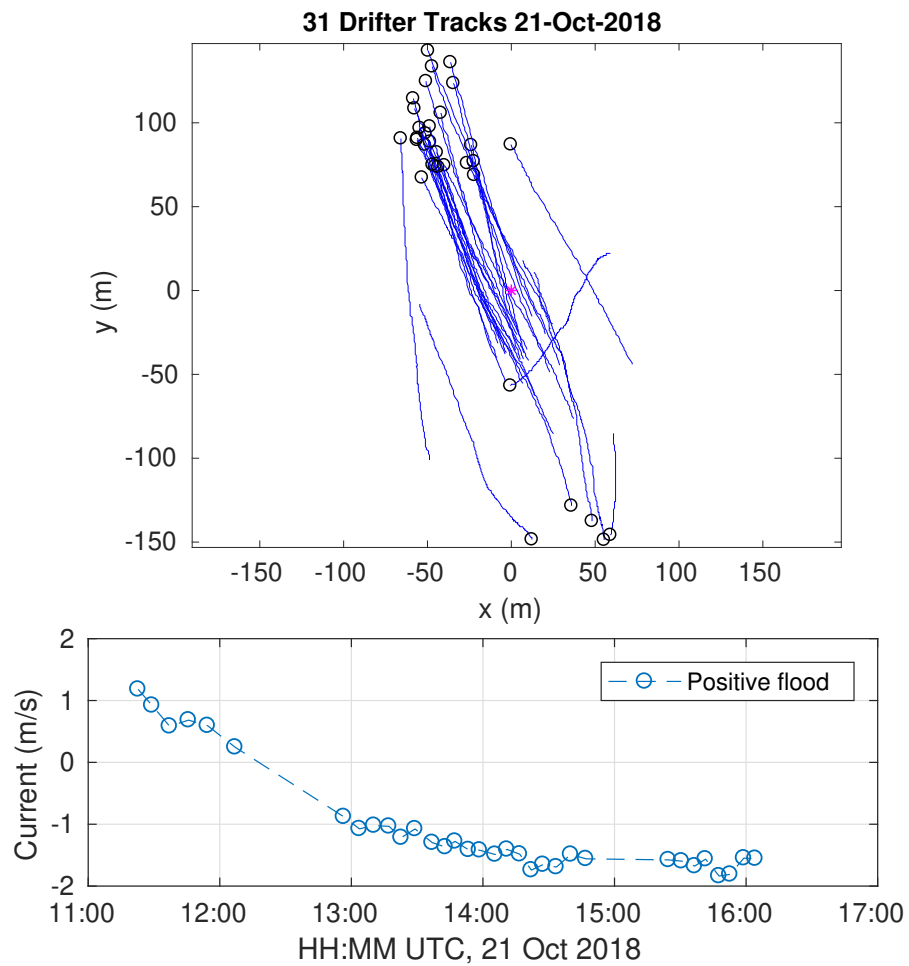


Figure 37: TOP: Tracks of the pad-float drifter relative to PLAT-I. The start of each drifter track is marked with a black circle. The magenta asterisk indicates the PLAT-I at the origin. BOTTOM: Current speed calculated from each drifter track.

as a potential hazard for the pad-float because the bows of the starboard and port hulls sometimes lifted clear of the water. A current meter (not ours) had been mounted on a pole from the bridge of PLAT-I. Unknown to the pad-float deployment team, the swell was lifting the current meter clear above the sea surface before plunging it back downwards. Remarkably, the pad-float drifted beneath the current meter while it was out of the water and was hit from above as the current meter plunged downwards with the swell. The pad-float hydrophone-array was tipped upside down but was otherwise unharmed. In future, we would only use the pad-float in calm conditions, as it was intended to be used.

The pad-float array successfully negotiated a path between the hulls and Schottel Deployment Modules (SDMs) of PLAT-I without any damage to hydrophones. This included trajectories in which the pad-float was on a direct heading for an SDM. Again, the pad-float remained stable as it bumped into the SDM and then rotated safely around it. The smallest gap (a little more than 0.9 m) is between the outer SDMs and the outer hulls. The pad-float remained stable as it negotiated that gap.

Figure 37 shows only those portions of the drifter tracks when hydrophone measurements were deemed reliable. That is to say, when the boat engine was shut down. Tracks were obtained on the flood tide at first (northwards motion), and later on the ebb tide (Table 1). The duration of each track is small compared to tidal time scales, so the lower panel of Figure 37 shows average current speed for each drift. All measured current speeds were less than 2 m/s.

## 5.2 Compass performance on PLAT-I

A pad-float passing close to the steel hulls of PLAT-I (right panel of Figure 36) raises a question as to how well the compass will work in order to establish orientation of the hydrophone array. On 8 November 2018 we tested the Aaronia GPS/compass by mounting it 2 m above deck level on the aluminum mast at the bow of PLAT-I (Figure 13). Another GPS unit was mounted near the stern of PLAT-I. Comparing compass headings with headings derived from separated GPS positions (Figure 38) showed reasonable agreement for a portion of the turn of the tide (magenta) but a very poor result (blue) otherwise.

In view of unreliable compass performance on PLAT-I, it is not advisable to use a compass to measure the orientation of the pad-float because some of the most important measurements to be made by the hydrophones on the pad-float are made close to the steel hulls of PLAT-I. The most reliable method for obtaining the orientation of the pad-float would be to have an icTalk mounted on PLAT-I so that transmitted signals from the known location provide a reference direction.

## 5.3 PSD from the pad-float hydrophone measurements

The 21 October 2018 pad-float measurements were not made in calm conditions so waves slapping on the pad-float may have somewhat contaminated the hydrophone measurements. Nevertheless, it may be useful to calculate the power spectral density (PSD) obtained from those measurements. Sampling rate of the hydrophones was 512 kS/s. PSD were calculated using the Welch method. The number of points in the FFT was  $N = 2^{18}$  samples, a hanning window was applied to minimize leakage, and a 50% overlap was used. PSD were averaged over all three hydrophones for the duration of each drift.

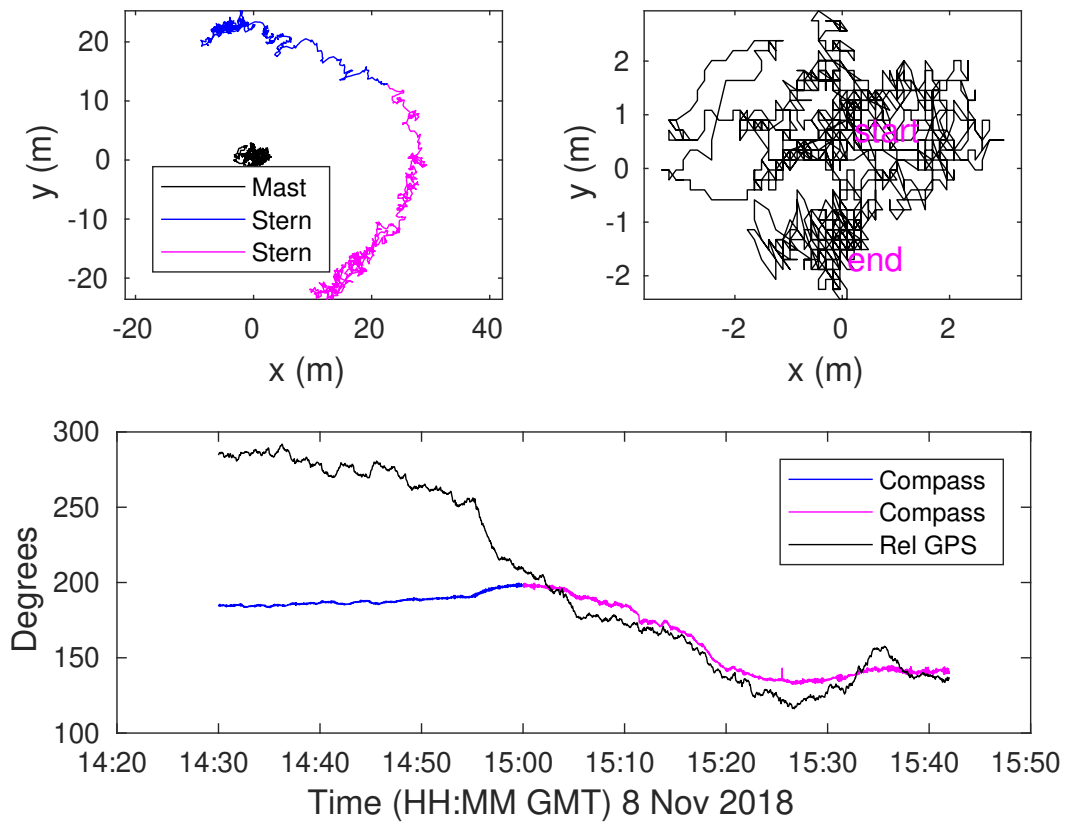


Figure 38: Testing the Aaronia GPS/compass as PLAT-I turns with a change of the tide.

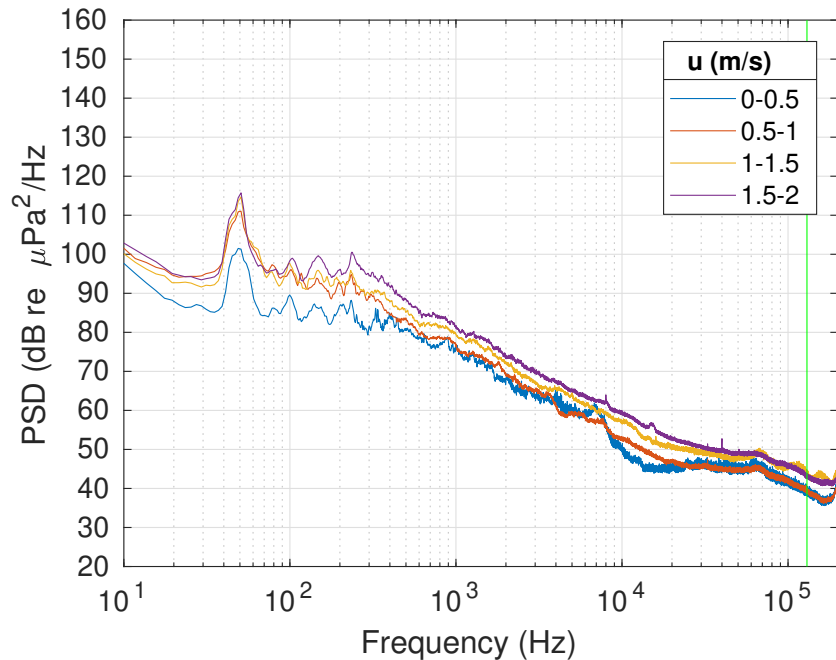


Figure 39: PSD obtained from the pad-float drifter array on 21 Oct 2018. Only considered drifts near PLAT-I. Drifts 13, 17, 19, 24 were excluded because they appeared to have anomolous variability. Averaged over all three hydrophones and duration of each drift. Then averaged results into bins according to current speed.

Figure 39 shows PSD averaged over bins according to current speed. Comparing with measurements obtained at the FORCE Test Site (Figure 28) we see that the band of frequencies that porpoise use has similar levels when current speed is less than 1 m/s. When tidal currents run fast, the high-frequency sound level at the FORCE Test Site becomes much larger than near the PLAT-I installation at Grand Passage. This is as expected, given that peak current speeds are three times larger at the FORCE Test Site.

#### 5.4 Environmental Effects Monitoring Hydrophone on PLAT-I

Sustainable Marine Energy mounted an icListenHF hydrophone to PLAT-I as a part of the Environmental Effects Monitoring Plan (EEMP). The hydrophone was attached to the base of a mount (Figure 40) designed and constructed in October 2018 for the Aris sonar, while undertaking STREEM field work. The Aris mount was used for measurements reported above §3.2.1. The resulting configuration placed the hydrophone at a level just below the bottom of the port hull. This was a far from optimal mount system for a hydrophone, given the strong disturbance of the flow associated with the breaking bow wave of the port hull and the high flow disturbance that the mount poles caused near the air-water interface.

The original intent of STREEM had been to analyse some of the hydrophone measurements made for the EEMP. To reduce flow disturbance, and to place the hydrophone well below sound sources resulting from flow disturbance, it would have been better for the EEMP to use a third-generation mount (a modified version of the second-generation mount shown in Figure 15). Regardless, some of the measurements made by the EEMP hydrophone are analysed

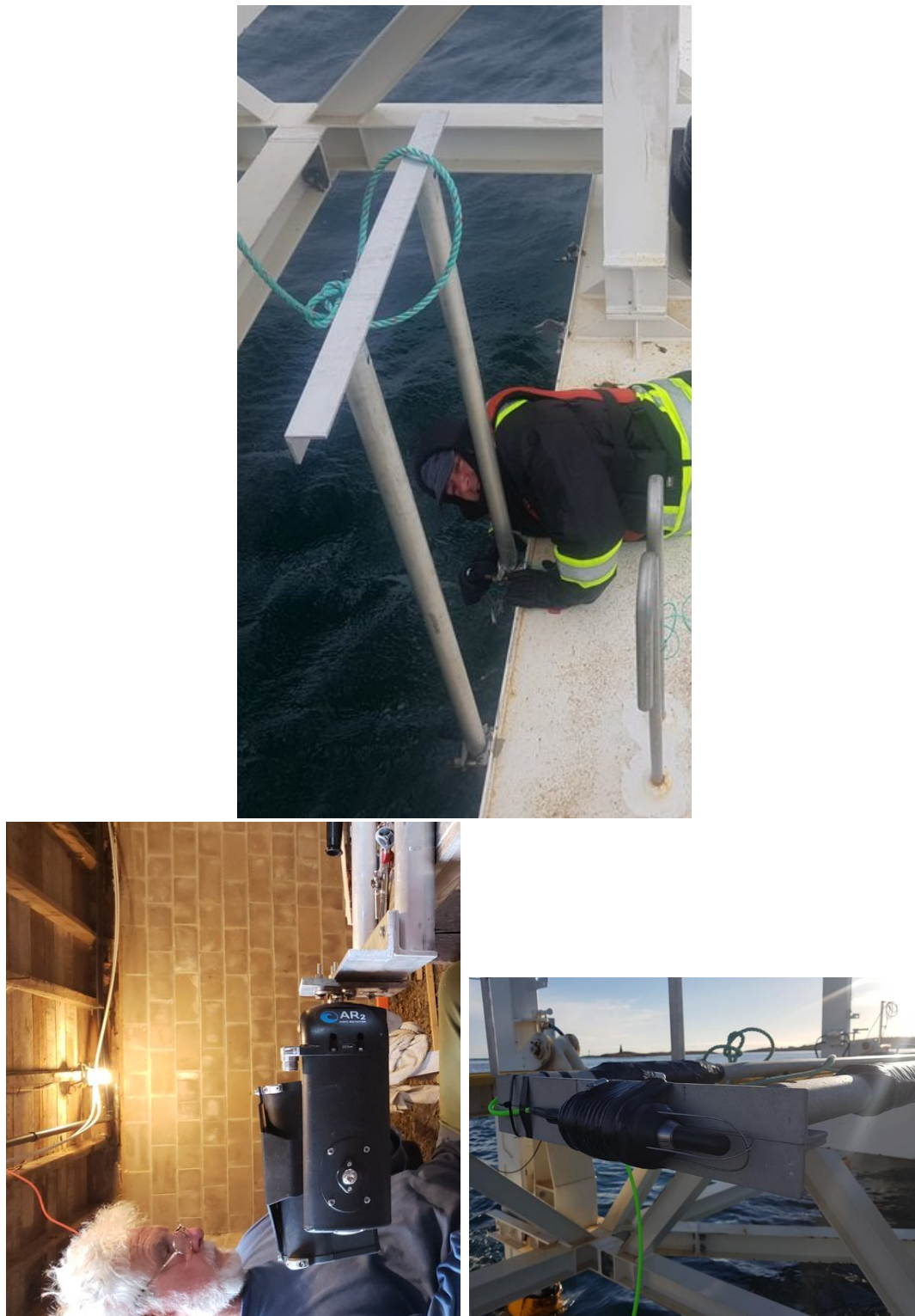


Figure 40: TOP: View of the upper portion of the Aris mount as it is being bolted onto the starboard hull of PLAT-I. BOTTOM LEFT: View of the Aris sonar/robot being fitted to the lower portion of the Aris mount. BOTTOM RIGHT: The Aris sonar/robot was replaced with an icListenHF hydrophone for Environmental Effects Monitoring by Sustainable Marine Energy (SME). Photo credit: Mike Adams and Greg Trowse.

below.

#### 5.4.1 PSD of the Environmental Effects Monitoring Hydrophone on PLAT-I

EEMP hydrophone measurements made from PLAT-I in late November and early December 2018 were made available for *STREEM*. Only measurements made on 29 November 2018 will be discussed in detail. These measurements were made during the EEMP commissioning stage, before turbine rotors were installed.

Power spectral density (PSD) were calculated for the full 24 hours (GMT) of 29 October. PSD were averaged over 10 minute segments. A full exposition of those 10 minute segments will not be presented here. Nevertheless, top plot in Figure 41 shows the daily-average PSD (black line) as well as minimum and maximum PSD obtained from the 10 minute averaged PSD. The PSD minimum (blue line) might be considered to be representative of slack tide and the maximum of the strongest part of the tidal flow. Several important matters are immediately apparent.

First, is the spectral peak at 150 Hz. On 29 November 2018, the peak appears to be most prominent when the tide is running (black and brown lines in Figure 41) but further investigation showed that this peak had nothing to do with the tide. A 150 Hz tone is perfectly audible. Listening to measurements on 29 November 2018 and viewing spectrograms, showed that the 150 Hz tone was evident only when the flood tide was running. The ebb tide was more characterized by hull banging and trickles extending to higher frequencies. At slack tide there was hull banging and some trickles with little high frequency energy. Audio files have been created to hear the 150 Hz tone and other sounds recorded by the EEMP hydrophone (Table 4). Subsampled measurements from other days showed that the 150 Hz tone could be present — or not present — during any stage of the tide.

Wind is the most likely cause of the 150 Hz tone. EEMP monitoring used pipes to mount instruments. Typically, these pipes had a substantial part of their length above water level. A pipe with one end open and the other closed by being in the water becomes a quarter-wave resonator. Thus wind blowing over the open end might be expected to produce a tone, corresponding to a resonant mode. The frequency  $f$  of the tone depends upon the length  $L$  of pipe above water

$$f = n \frac{c_{\text{air}}}{4L} \quad (2)$$

where  $c_{\text{air}} \approx 340$  m/s is the speed of sound in air and the mode number  $n = 1, 3, 5, \dots$  is an odd integer. A pipe length  $L = 1.7$  m would result in air in the pipe having a resonant frequency of 150 Hz for the  $n = 3$  mode. Given the relatively large acoustic impedance of water relative to air, such resonant sound would propagate very efficiently into the water.

The top panel of Figure 40 shows pipes that are capped by angle aluminum. Nevertheless, there are gaps and also a bolt access hole that might allow excitation of a resonant mode. Other poles, used for cameras, had totally open ends.

Audiograms have been obtained for some species of fish [42, 43] although not, perhaps, for all the species that may be of interest in Grand Passage. Given what is known about fish audiograms, it seems quite likely that some species detect the strong 150 Hz tone that is apparent in Figure 41. The possibility that such a tone might modify marine animal behavior cannot be discounted.

Figure 41 shows that the sound level varies greatly with tide for frequencies utilized by harbour porpoises. Indeed, averaged sound level in the 60-70 dB range is observed for flood

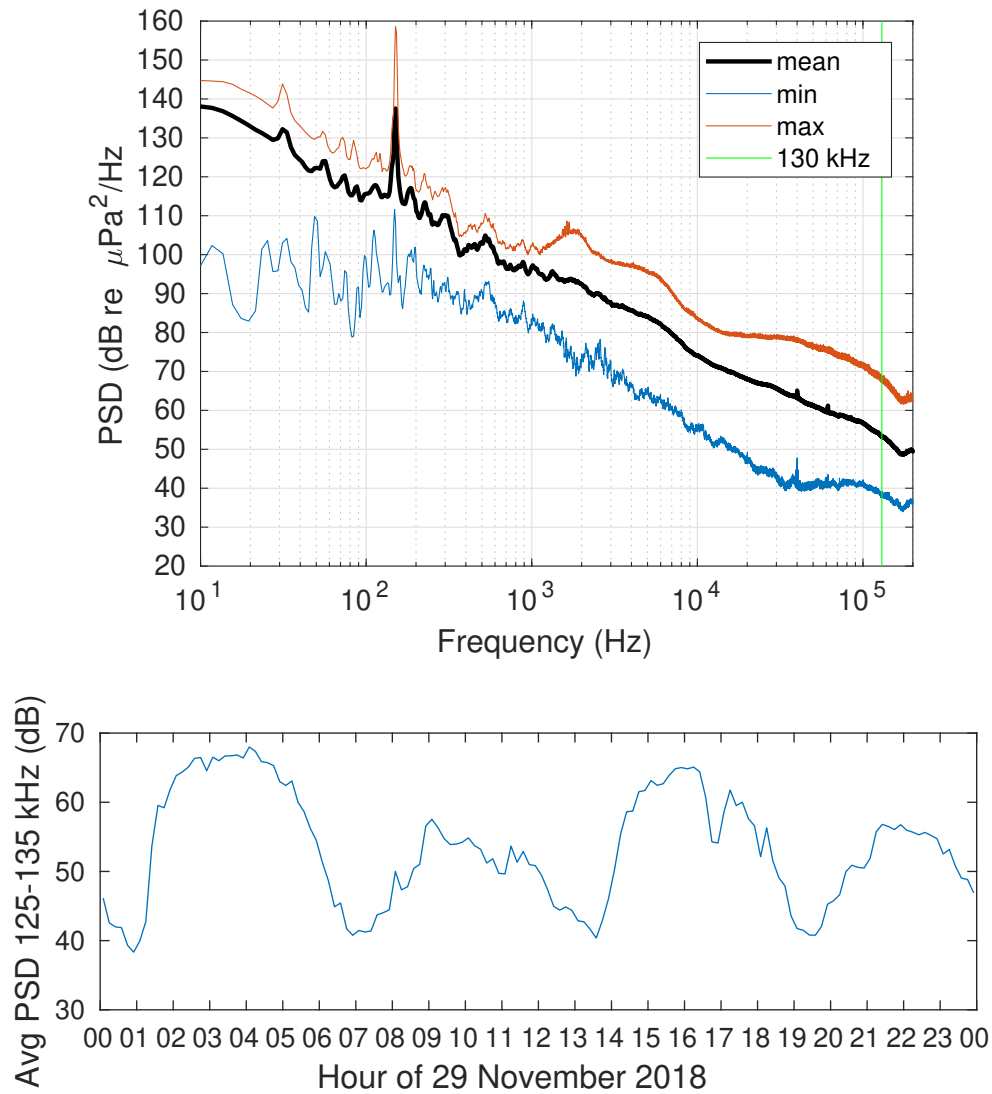


Figure 41: TOP: PSD obtained from the environmental monitoring hydrophone on PLAT-I. Brown/blue represents the maximum/minimum of 10-minute averaged spectra, black is the average of spectra over the full 24 hours. BOTTOM: Timeseries of PSD averaged in the frequency range 125-135 kHz. PSD were calculated using the Welch method. Sample frequency is 512 kS/s, number of points in FFT was  $N = 2^{18}$  samples, 50% overlap, hanning window, and spectral estimates were subsequently averaged over 10 minutes. Measurements are from the entire day of 29 November 2018.

File	Tide	Sound
PLAT-I_20181129_033000.mp3	flood	trickles and 150 Hz tone
PLAT-I_20181129_070000.mp3	slack, high tide	hull banging and trickles
PLAT-I_20181129_110000.mp3	ebb	hull banging and trickles
PLAT-I_20181129_170000.mp3	flood	trickles and 150 Hz tone
PLAT-I_20181129_233000.mp3	ebb	hull banging and trickles

Table 4: Audio files created from measurements made on 29 Nov 2018 by the Environmental Effects Monitoring icListenHF hydrophone that was mounted to PLAT-I. The 150 Hz tone may correspond to a resonance of the mount pole.

tides (Table 1). Such sound levels are more extreme than those measured at the FORCE Test Site (Figure 28). Current speeds are three times larger at the FORCE Test Site. High sound levels measured by the EEMP hydrophone on PLAT-I are most likely caused by the mounting arrangement and proximity to water disturbance by PLAT-I.

Such high sound levels might be expected to make it more difficult to reliably detect vocalizations of marine mammals. Nevertheless, *STREEM* has analysed the 29 November measurements to see if clicks from harbour porpoises could be detected.

#### 5.4.2 Detections of Harbour Porpoise Vocalizations

The Coda click detector was used to identify times at which the 29 November 2018 EEMP hydrophone may have recorded vocalizations by harbour porpoises. Potential detections were visually reviewed using spectrograms and more sophisticated mathematical techniques.

The left spectrogram in Figure 42 is a straightforward visualization of a click train detected near slack water at low tide. Such click trains are very evident within a spectrogram when ambient sound levels are low.

It must be emphasized that the sound levels shown in Figure 41 represent values averaged over time periods much longer than the duration of a porpoise click train. Over short time intervals, sound levels may be much higher or much lower than those averaged values. Thus, the left spectrogram in Figure 42 is a brief interval when sound level is low. The right spectrogram in Figure 42 shows a brief interval when sound level is much higher. This spectrogram shows broad band noise structures, extending from lower frequencies that are within the audible range of humans to very high frequencies that are above the audio range of harbour porpoises. One must zoom in on such spectrograms in order to find visual evidence for the porpoise clicks which Coda detected. The evidence is there, but it would be extremely difficult to find without Coda.

The top left spectrogram in Figure 43 shows a brief time interval when there is a lot of high frequency sound which is disconnected from low frequency sounds. This is early in the flood tide, when averaged sound levels are relatively high (Figure 41). Again, it is impossible to visualize the clicks which Coda detects without zooming to resolve the spectrogram in great detail. The top right spectrogram clearly shows a click train late on the flood tide, but brief interval when ambient sound level is low. The bottom left spectrogram shows a click train detected on the ebb tide.

Over the entire day, the percentage of detection positive minutes was 9.4%. Detection positive minutes are strongly clustered, being much more common near the first 3 hours of

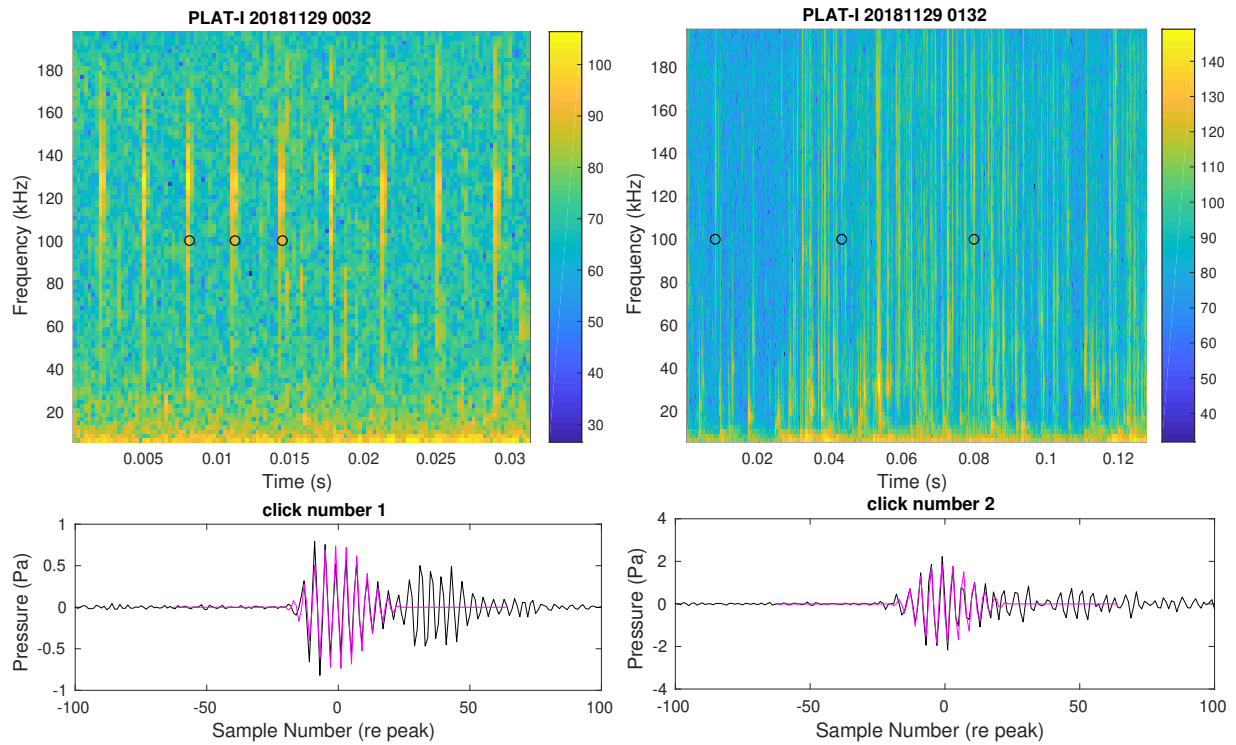


Figure 42: TOP: Spectrograms with black circles indicating times when clicks were detected on 29 November 2018. BOTTOM: Clicks fitted (magenta) to the filtered timeseries (black).

the flood tide (Figure 43, lower right). Given that typical swimming speed of a porpoise is 1 m/s, we expect that they would be moved back and forth, to some extent, by the tide. One should not jump to a conclusion that the pattern of porpoise vocalization activity seen on 29 November 2018 is representative of a general pattern.

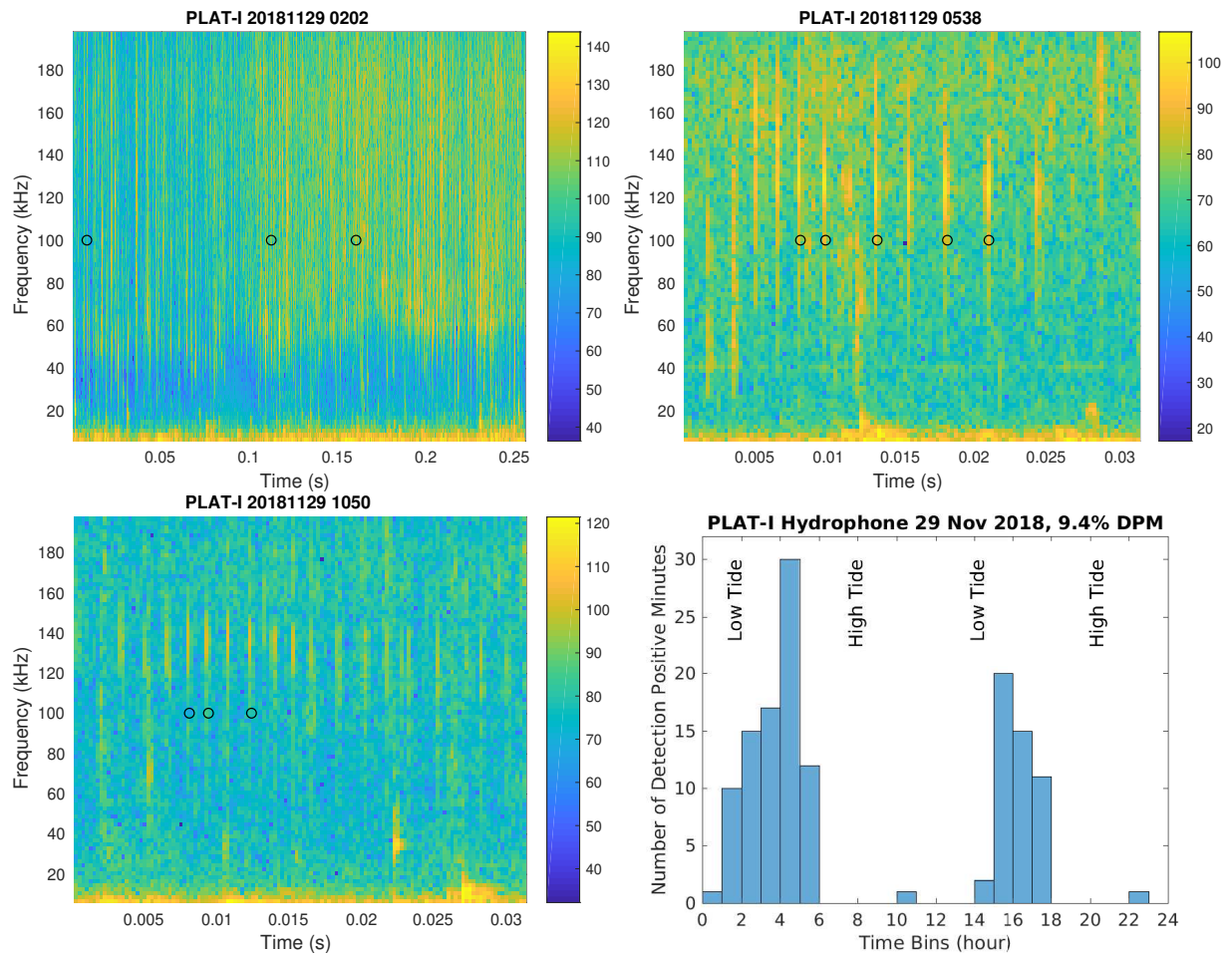


Figure 43: Spectrograms with black circles indicating times when clicks were detected. Histogram showing the number of detection positive minutes (DPM) during each hour (UTC).

## 6 Summary Points

1. Our method of boat-mounted imaging sonar and a target-drifter showed promise for testing detection of targets as a function of range, depth, orientation and position within the sonar beam. Careful attention must be given to the following factors. (a) Apparatus must be designed without unwanted targets (i.e. thin lines, no reflective fittings, deep weight/spreading bar). (b) Measurements must be done in calm conditions with slow currents and sufficiently deep water in order to precisely control boat orientation and position and avoid spurious reflections. (c) The boat mount must be capable of deploying instruments to depths of at least 5 m and be easy to raise and lower. See §3.1.
2. The Gemini 720is imaging sonar reliably detected fish and fish-like targets over a wide field of view. See §3.1 and §3.2.
3. It is unreasonable to expect the Gemini 720is imaging sonar to enable identification of fish or fish-like targets except by context (location, season and additional measurements/information) and size. See §3.1.1, §3.1.2, §3.2.1, and §3.2.2.
4. The Gemini 720is imaging sonar detected a school of fish about 15 m from a turbine hub and in the depth range spanned by the turbine rotor. See §3.2.2.
5. The Gemini 720is could be rotated to obtain depth and range of targets, although the signal was complicated by ghost images caused by beam paths reflected off the sea surface; §3.2.4. Application of a rotated Gemini should be restricted to deep water installations. The Aris has a much more narrow angular field of view, so it would best serve for a rotated application to obtain range and depth of targets near PLAT-I turbines in Grand Passage. See §3.2.4.
6. The Gemini 720is and Aris imaging sonars can be operated together without one causing interference for the other. See §3.2.1.
7. Strong reflections cause side lobes that degrade Gemini images in the angular dimension (equation 1). PLAT-I infrastructure caused such reflections. See §3.2.1.
8. The Gemini 720is detected and track targets that are on the other side of zones where PLAT-I infrastructure degraded Gemini performance. See §3.2.3.
9. With a different mounting arrangement, the Gemini could be operated on PLAT-I without image contamination caused by reflections off PLAT-I infrastructure. See §3.2.5.
10. The Aris sonar reliably detected a fish target but only over a narrow field of view. The Aris sonar does not allow target identification, except by context (movement, location, season and additional measurements/information) and size. See §3.2.1.
11. An optical camera reliably detected a fish target and images were sometimes sufficient for identification; §3.2.1. However, optical cameras have a very limited field of view so they must be placed very close to the area to be monitored in order to be effective; §3.2.1. Rapid biofouling requires cameras be frequently serviced in Grand Passage.

12. A configuration of imaging sonars and optical cameras has been designed for PLAT-I in order to effectively monitor fish-turbine interaction. See §3.2.2 and §7.
13. The Gemini 720is imaging sonar emits pulsed signals that appear in the spectra obtained from icListenHF hydrophones at frequencies from 50-256 kHz. See §4.1.
14. A small (length 22 mm) Vemco 180/170 kHz fish tag is well detected by the Gemini 720is imaging sonar when the tag is not transmitting. See §3.1.2.
15. 180 kHz transmissions from a Vemco 180/170 kHz acoustic fish tag caused false detections by the Gemini 720is. Those false detections had distinctive structure and were infrequent. See §4.1.4.
16. Performance of a Vemco HR2 receiver was not impacted by an operating Gemini 720is. See §4.1.5.
17. A Vemco HR2 receiver was mounted to PLAT-I and it reliably detected both PPM and HR signals from an acoustic tag. The HR2 receiver was set at a depth of 3.5 m using our second-generation mount. Good performance cannot be expected unless the mount system locates the receiver well away from surfaces that reflect acoustic signals. See §4.2.1.
18. Echosounders and fish finders cause disruptive false signals in Gemini 720is images. See §4.2.2.
19. Echosounders and fish finders disrupt collection of high frequency hydrophone measurements. They may also be disruptive to some marine mammals. See §4.2.3. Local whale tour vessels turn off echosounders when whales are nearby.
20. Service vessels should not use echosounders and fish finders when environmental effects monitoring is being done nor when scientific measurements are being made.
21. The pad-float drifter with hydrophone array showed considerable promise for measuring sound at and around a floating turbine installation like PLAT-I. See §5.1 and §5.3.
22. Unreliable compass performance on PLAT-I indicates that an icTalk should be used for obtaining orientation of the pad-float hydrophone array. See §5.2.
23. A strong 150 Hz signal was found in the measurements made by an environmental effects monitoring program (EEMP) icListenHF hydrophone that was mounted to PLAT-I. This signal was consistent with wind exciting resonant sound oscillations inside poles used to mount the EEMP equipment. See §5.4.1.
24. The EEMP hydrophone was attached to PLAT-I using an inadequate mounting system and this caused excessive noise to be recorded. See §5.4.1.
25. One day of EEMP hydrophone measurements was analyzed. 9.4% of the minutes were detection positive for harbour porpoise click trains. See §5.4.2.

## 7 Comments on Monitoring to Assess Risk

*What risk does a turbine mounted to PLAT-I pose to marine animals in Grand Passage?*

Suggestions made previously §3.2.5 for effective monitoring of fish-turbine interaction go some distance towards resolving this question. Multiple sonars can detect and track targets approaching from upstream (Figure 24). Detections far upstream provide a means to estimate encounter rates. Trajectories will show any avoidance behaviour by approaching targets, either by vertical or horizontal movements so that targets pass clear of the area swept by the turbine. This is very useful for assessing risk to marine animals. Importantly, such measurements can be achieved day and night.

Marine life targets that show no avoidance behaviour — or are attracted to the turbine — might at least be identified as they pass within the volume measured by both sonars and upstream facing optical cameras. There is a likelihood of semi-automating target detection and tracking by using cameras and sonar facing upstream. Semi-automated detections in images looking upstream indicate when human effort might be most profitably applied to find targets in more complex images obtained from cameras that have turbine rotors in their field of view.

Some degree of semi-automated target detection is required in order to achieve a practicable method for resolving the question of risk. One thing that *STREEM* makes abundantly clear is the need for high quality instrument mounting systems so that monitoring equipment can be positioned in the optimal way in order to be most easily serviced and to provide the highest possible quality of data. Good data analysis begins with good measurements and good measurements begin with good experimental design and excellent instrument deployment.

Downstream, where water is swept by the turbine blades, the task becomes much more difficult to semi-automate. At least the identification of targets by the upstream sensors will guide efforts to examine the visual record of a fish being struck (or not) by rotating blades. A camera may or may not be able to resolve any visible physical damage. But not even in principle can a camera inform us of the fish's fate with regards to damage done by a glancing blow, by shear stresses, or by pressure changes.

With the technologies that we have at hand, the best hope of resolving the question is to:

- Measure how many fish are approaching from upstream when the turbine is rotating fast.
- Measure what fraction, of those fish that do approach, are subsequently seen to avoid the area swept by the turbine blades. Thus, sonar (perhaps also echosounders) would seem to be indispensable for measuring an upper limit on whatever risk that turbines pose to fish.

On the other hand, signals emitted by sonar and other active acoustic devices may change the behaviour of alosine herring [41] and marine mammals [29, 39, 40]. Thus, key methods used for addressing the risk of turbines to many species of fish are confounding for addressing the risk to marine mammals (and alosine herring, perhaps).

Nevertheless, optical methods applied for fish detection are also applicable for observing any localized interaction of marine mammals with turbine infrastructure. Detections of vocalizations [15, 14] and localization [16, 44] are the most likely methods for providing continuous information about marine mammal identity and abundance beyond the view of cameras. Trained observers may identify marine mammals but only during daylight hours when conditions are calm and clear. Cameras mounted to drones would be useful for obtaining optical measurements over a broad area. Combined, these techniques might, at least in principle, quantify bounds on the extent that turbines may or may not affect marine mammals.

Results thus far — ours and others [29, 39, 40, 41] — show that some measurement methods interfere with others and probably also interfere with some species. Whenever possible, it is best to avoid contaminating factors and that often requires an experimental approach that addresses one problem at a time.

## 8 Acknowledgments

Mike Adams assisted with all aspects of the field program. Greg Trowse captained RV Puffin and assisted in field activities and planning. Eric Bibeau contributed the Aris imaging sonar and assisted in the field. Acadia University provided significant equipment, including two icListenHF hydrophones and the Gemini imaging sonar. Dalhousie University provided access to an additional icListenHF hydrophone. SME provided access to PLAT-I for testing environmental monitoring instruments and SME engineers coordinated activities on site with STREEM researchers. We are grateful to the Offshore Energy Research Association and the Nova Scotia Department of Energy and Mines for contributing project funding.

## References

- [1] Price, D. 1995. Energy and human evolution. *Population and Environment*, 16(4), 301-319.
- [2] IPCC Fourth Assessment Report: Climate Change 2007.  
<https://www.ipcc.ch/assessment-report/ar4/>
- [3] May, R.M. 2010. Ecological science and tomorrow's world. *Philosophical Transactions of the Royal Society B* 365, 41-47. doi:10.1098/rstb.2009.0164
- [4] Dietrich, D.E., Bowman, M.J., Kolankiewicz, L., & Sanderson, B.G. 2017. Much Faster Sea Level Rising Ahead! *J. Sustainable Energy Eng.*, 5(3): 207-211.
- [5] The Shift Project. Data Source: The World Bank - World Development Indicators  
<http://www.tsp-data-portal.org/Breakdown-of-Electricity-Generation-by-Energy-Source>
- [6] McCully, P. 2001. *Silenced Rivers: The Ecology and Politics of Large Dams*. Zed Books.
- [7] Hawley, S. 2012. *Recovering a Lost River: Removing Dams, Rewilding Salmon, Revitalizing Communities*. Beacon Press.
- [8] Lavin, M. F., Godinez, V. M., & Alvarez, L. G. 1998. Inverse-estuarine Features of the Upper Gulf of California. *Estuarine, Coastal and Shelf Science* 47, 769-795.  
<https://doi.org/10.1006/ecss.1998.0387>
- [9] Dadswell, M.J., & Rulifson, R.A. 1994. Macrotidal estuaries: a region of collision between migratory marine animals and tidal power development. *Biological Journal of the Linnean Society*. 51, 93-113

- [10] Karsten, R., McMillan, J., Lickley M., & Haynes R. 2008. Assessment of tidal current energy in the Minas Passage, Bay of Fundy. *Journal of Power and Energy*, Vol. 222 (A3), pp. 289-297.
- [11] Keyser, F. M., Broome, J. E., Bradford, R. G., Sanderson, B. G. and Redden, A. M. 2016. Winter presence and temperature-related diel vertical migration of Striped Bass (*Morone saxatilis*) in an extreme high flow site in Minas Passage, Bay of Fundy. *Can J Fish Aquat Sci*, 73, 1777-1786.
- [12] Stokesbury, M.J.W., Logan-Chesney, L.M., McLean, M.F., Buhariwalla, C.F., Redden, A.M., Beardsall, J.W., Broome, J., Dadswell M.J., 2016. Atlantic sturgeon spatial and temporal distribution in Minas Passage, Nova Scotia: a region of future tidal power extraction. *PLoS One*, 11 (7), e0158387. doi:10.1371/journal.pone.0158387
- [13] Sanderson, B., Buhariwalla, C., Adams, M.J., Broome, J., Stokesbury, M., & Redden, A.M. 2017. Quantifying detection range of acoustic tags for probability of fish encountering MHK devices. *European Wave and Tidal Energy (EWTEC) 2017 Conference*. Cork, Ireland. pp. 10
- [14] Tollit, D., Joy, R., Wood, J., Redden, A., Booth, C., Boucher, T., Porskamp, P., & Oldreive, M. 2019. Baseline presence of and effects of tidal turbine installation and operations on harbor porpoise in Minas Passage, Bay of Fundy, Canada. *Journal of Ocean Technology* (in press).
- [15] Adams, M.J., Sanderson, B.G., Porskamp, P., & Redden, A.M. 2019. Comparison of co-deployed drifting passive acoustic monitoring tools at a high flow tidal site: C-PODs and icListenHF hydrophones. *Journal of Ocean Technology* (in press).
- [16] Sanderson, B.G., Adams, M.J., & Redden, A.M. 2019. Using reflected clicks to monitor range and depth of Atlantic harbour porpoise. *Journal of Ocean Technology* (in press).
- [17] Fisheries Act, 1985, R.S., c. F-14, s. 1.
- [18] ISEM 2019. Integrated Active and Passive Acoustic System for Environmental Monitoring of Fish and Marine Mammals in Tidal Energy Sites (ISEM). OERA project reference: 300-173-2.
- [19] Sanderson, B. & Redden, A.M., 2016. Use of fish tracking data to model striped bass turbine encounter probability in Minas Passage. Final Report to the Offshore Energy Research Association of Nova Scotia. ACER Technical Report No. 122, 54 pp, Acadia University, Wolfville, NS, Canada.
- [20] Lossent, J., Lejart, M., Folegot, T., Clorennec, D., Di Iorio, L., and Gervaise, C. 2018. Underwater operational noise level emitted by a tidal current turbine and its potential impact on marine fauna. *Marine Pollution Bulletin*, Vol. 130, pp. 323-334
- [21] Viehman, H.A., Zydlewski, G.B. 2015. Fish Interactions with a Commercial-Scale Tidal Energy Device in the Natural Environment *Estuaries and Coasts* (2015) 38 (Suppl 1):S241S252 DOI 10.1007/s12237-014-9767-8

- [22] Williamson, B.J., S. Fraser, P. Blondel, P.S. Bell, J.J. Waggitt, and B.E. Scott. 2017. Multisensor acoustic tracking of fish and seabird behavior around tidal turbine structures in Scotland. *IEEE Journal of Oceanic Engineering*.
- [23] Hammar, L., Andersson, S., Eggertsen, L., Haglund, J., Gullstrom, M., Ehnberg, J., Molander, S. 2013. Hydrokinetic Turbine Effects on Fish Swimming Behaviour. *PLoS ONE* 8(12): e84141. doi:10.1371/journal.pone.0084141
- [24] Broadhurst, M.; Barr, S.; Orme, D. (2014). In-Situ Ecological Interactions with a Deployed Tidal Energy Device; An Observational Pilot Study. *Ocean & Coastal Management*, 99, 31-38.
- [25] Shen, H., Gayle Zydlewski, H. Viehman, G. Staines 2016. Estimating the probability of fish encountering a marine hydrokinetic device. *Renewable Energy*, 97, 746-756 <https://doi.org/10.1016/j.renene.2016.06.026>
- [26] Viehman, H.A., G.B. Zydlewski. 2015. Fish interactions with a commercial-scale tidal energy device in the natural environment. *Estuaries and Coasts*, 38 (Suppl 1):S241S252 DOI 10.1007/s12237-014-9767-8
- [27] Belcher, E., B. Matsuyama, G. Trimble. 2001. Object identification with acoustic lenses. *MTS* 0-933057-28-9
- [28] Colinvaux, P.A. 1978. *Why Large Fierce Animals are Rare: An Ecologist's Perspective*. Princeton University Press, Princeton, New Jersey.
- [29] Bernaldo de Quiros, Y., A. Fernandez, R. W. Baird, R. L. Brownell, N. Aguilar de Soto, D. Allen, M. Arbelo, M. Arregui, A. Costidis, A. Fahlman, A. Frantzis, F. M. D. Gulland, M. Iiguez, M. Johnson, A. Kommenou, H. Koopman, D. A. Pabst, W. D. Roe, E. Sierra, M. Tejedor and G. Schorr. 2018. Advances in research on the impacts of anti-submarine sonar on beaked whales. *Proceedings of the Royal Society B: Biological Sciences*, 286. <http://doi.org/10.1098/rspb.2018.2533>
- [30] Sanderson, B.G. 2018a. Drifter-Target Tests with Gemini, 19 Oct 2018.
- [31] Sanderson, B.G. 2018b. Gemini Detection of Targets on PLAT-I, 23 Oct 2018.
- [32] Sanderson, B.G. 2018c. Gemini with Vertical Orientation: 24 Oct 2018. Hypertext document describing experiments, results, and with links to movies and measurements.
- [33] Villadsgaard, A., Wahlberg, M., & Tougaard, J. 2007. Echolocation signals of wild harbour porpoises, *Phocoena phocoena*. *Journal of Experimental Biology*, 210: 56-64.
- [34] Linnenschmidt, M., Kloepper, L. N., Wahlberg, M., & Nachtigall, P. E. (2012). Stereotypical rapid source level regulation in the harbour porpoise biosonar. *Naturwissenschaften*, 99(9), 767-771.
- [35] Kyhn, L. A., Tougaard, J., Beedholm, K., Jensen, F. H.J, Ashe, E., Williams, R., & Madsen, P. T. (2013). Clicking in a killer whale habitat: narrowband, high-frequency biosonar clicks of harbour porpoise (*Phocoena phocoena*) and dall's porpoise (*Phocoenoides dalli*). *PloS one*, 8(5), e63763.

- [36] Porskamp, P.H.J., Broome, J.E., Sanderson, B.G., & Redden, A.M. 2015. Assessing the performance of two passive acoustic monitoring technologies for porpoise detection in a high flow tidal site. *Journal of the Canadian Acoustical Association* Vol. 43(3).
- [37] Sanderson, B., Mike Adams, M., & Redden, A. 2019. Application of Drifters with Suspended Hydrophone Arrays to Assess Harbour Porpoise Use of the Water Column and Spatial Overlap with MRE Devices in Minas Passage. Final Report to the Offshore Energy Research Association of Nova Scotia. ACER Technical Report #126, 63 pp, Acadia University, Wolfville, NS, Canada.
- [38] Strasberg, M. 1979. Non-acoustic noise interference in measurements of infrasonic ambient noise, *Journal of the Acoustical Society of America*. Vol. 66. pp. 1487-1493. doi:10.1121/1.383543
- [39] Wisniewska, D.M., Johnson, M., Teilmann, J., Siebert, U., Galatius, A., Dietz, R., and Madsen, P.T. 2018. High rates of vessel noise disrupt foraging in wild harbour porpoises (*Phocoena phocoena*). *Proceedings of the Royal Society B*, Vol. 285: 0172314. <https://doi.org/10.1098/rspb.2017.2314>
- [40] Mikkelsen, L., Hermannsen, L., Beedholm, K., Madsen, P. T., and Tougaard J. 2017. Simulated seal scarer sounds scare porpoises, but not seals: species-specific responses to 12kHz deterrence sounds. *Royal Society Open Science*. Vol. 4(7). doi: 10.1098/rsos.170286
- [41] Dunning, D.J., Q.E. Ross, P.G. Geodhegan, J.J. Reichle, J.K. Menezes, and J.K. Watson. 1992. Alewives avoid high-frequency sound. *North American Journal of Fisheries Management*, 12: 407-416.
- [42] Popper, A.N., and C.R. Schilt. Hearing and Acoustic Behaviour: Basic and Applied Considerations. In *Fish Bioacoustics*, Webb, J.F., R.R. Fay, and A.N. Popper (Eds). 2008, XIV, 322 p 85 illus., Hardcover. ISBN: 978-0-387-73028-8
- [43] Nedwell, J.R., B. Edwards, A.W.H. Turnpenny, and J. Gordon. 2004. Fish and marine mammal audiograms: A summary of available information. Prepared by Subacoustech Ltd., Hampshire, UK. Report 534 R 0214.
- [44] Malinka, C.E., Gillespie, D.M., Macaulay, J.D.J., Joy, R., and Sparling, C.E. 2018. First *in situ* passive acoustic monitoring for marine mammals during operation of a tidal turbine in Ramsey Sound, Wales. *Marine Ecology Progress Series*, Vol. 590, pp. 247-266. <https://doi.org/10.3354/meps12467>